Towards quantum topological data analysis: torsion detection

Nhat A. Nghiem^{1, 2, *}

¹Department of Physics and Astronomy, State University of New York at Stony Brook, Stony Brook, NY 11794-3800, USA ²C. N. Yang Institute for Theoretical Physics, State University of New York at Stony Brook, Stony Brook, NY 11794-3840, USA

Topological data analysis (TDA) has become an attractive area for the application of quantum computing. Recent advances have uncovered many interesting connections between the two fields. On one hand, complexity-theoretic results show that estimating Betti numbers—a central task in TDA— is NP-hard, indicating that a generic quantum speedup is unlikely. On the other hand, several recent studies have explored structured, non-generic settings and demonstrated that quantum algorithms can still achieve significant speedups under certain conditions. To date, most of these efforts have focused on Betti numbers, which are topological invariants capturing the intrinsic connectivity and "holes" in a dataset. However, there is another important feature of topological spaces: torsion. Torsion represents a distinct component of homology that can reveal richer structural information. In this work, we introduce a quantum algorithm for torsion detection—determining whether a given simplicial complex contains torsion. Our algorithm, assisted by a classical procedure (for diagonalizing small integer matrix) of low complexity, can succeed with high probability and offer polynomial speed-up (in non-oracle setting) to exponential speedup (in oracle-setting) over the best-known classical approach.

I. INTRODUCTION

As an application of quantum theory—a scientific revolution of the early twentieth century—quantum computation has emerged as a powerful computing paradigm. Considerable effort has been devoted to exploring its potential, leading to many landmark algorithms and results [1–17]. More recently, there has been a surge of interest in applying quantum computation to topological data analysis (TDA)—a relatively young but rapidly growing field that uses tools from algebraic topology to study large-scale, complex data. Although TDA offers powerful insights, its methods can be computationally expensive, motivating the search for faster alternatives. Quantum computing, with its ability to manipulate high-dimensional states efficiently, has been viewed as a promising route to overcoming some of these computational challenges.

The interplay between quantum computing and TDA has already produced several interesting results. Lloyd, Garnerone, and Zanardi [18] introduced the first quantum algorithm (often called the LGZ algorithm) for estimating Betti numbers, one of the central invariants in TDA. Subsequent works [19–21] improved the LGZ framework in various ways. Hayakawa et al. [22] proposed a quantum method for estimating persistent Betti numbers, a more refined invariant. Others have examined the complexity-theoretic aspects of Betti number computation [23, 24]. Recent studies [25, 26] further demonstrate that, for certain classes of simplicial complexes, quantum algorithms can outperform previous approaches [18–20].

While most of these works focus on Betti numbers, they capture only part of the topological information. For a given simplicial complex, the Betti numbers measure the rank of the free part of the homology group. However, homology also contains another component: torsion. Intuitively, Betti numbers count the number of independent "holes" or cycles that cannot be filled, whereas torsion measures those cycles that become trivial (i.e., contractible) after a finite number of traversals. Together, the free part and the torsion part give a more complete characterization of a topological space. For example, a sphere and a Klein bottle differ not only in their Betti numbers but also in that the Klein bottle has torsion while the sphere does not. Yet, most existing TDA algorithms, classical or quantum, typically work over \mathbb{R} or \mathbb{Z}_2 , effectively hiding torsion information. Readers interested in a more formal discussion of this issue are referred to Appendix \mathbb{D} , which explains how the choice of coefficients can obscure torsion.

Motivated by this gap, our work explores the potential of quantum computation for torsion detection. Specifically, given a simplicial complex K, we ask: Does K contain torsion? Our algorithm draws on several mathematical tools. The key theoretical foundations are classical results from algebra, including the structure theorem for finitely generated abelian groups and the universal coefficient theorem, both of which imply that torsion is reflected in the dimensions of certain homology groups. Thus, our strategy reduces to estimating the dimensions of these groups—a task for which we propose a quantum procedure. Our method builds on recent advances in state preparation, block-encoding,

^{*} nhatanh.nghiemvu@stonybrook.edu

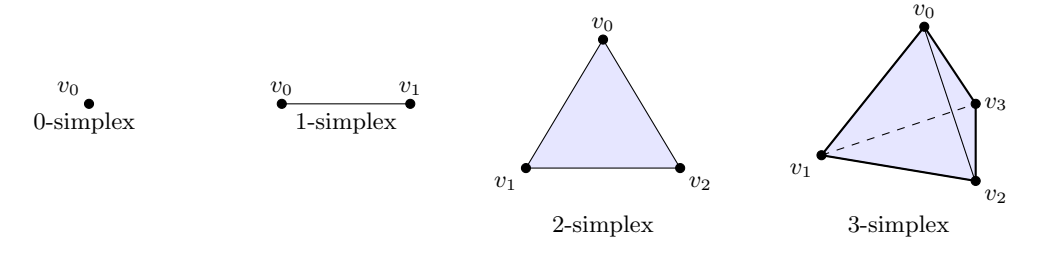


FIG. 1: Illustration of standard simplexes. From left to right: a point (0-simplex), a line segment (1-simplex), a filled triangle (2-simplex), a filled tetrahedron (3-simplex). Each r-simplex is formed by (r+1)-geometrically independent vertices in Euclidean space.

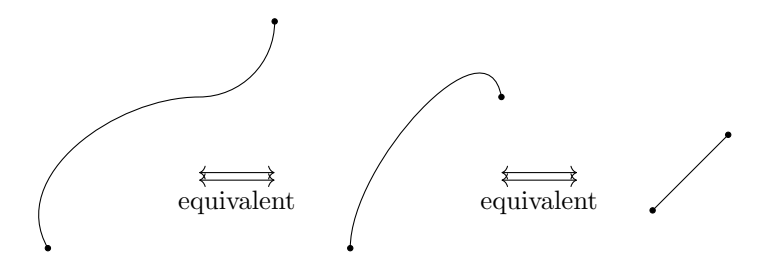
and the quantum singular value transformation (QSVT) framework. We show that, with suitable input, a quantum computer can detect torsion significantly faster than known classical algorithms.

The rest of the paper is organized as follows. Section II provides a brief introduction to TDA. Section III surveys the state-of-the-art quantum algorithms for TDA. Section IV presents our main contribution: a quantum algorithm for torsion detection. We conclude in Section V with broader reflections and future directions. Several appendices contain detailed material: Appendix A reviews block-encoding and related techniques; Appendix B summarizes algebraic background; Appendix C reviews topological concepts; Appendix D elaborates on the role of coefficient fields; Appendix F develops the main insight behind our method; Appendix G gives the full algorithm; and Appendix H provides a detailed complexity analysis.

II. TOPOLOGICAL DATA ANALYSIS

In this section, we provide an overview of topological data analysis (TDA), particularly its mathematical background. We keep things concise, intuitive and neat here and refer the interested readers to the Appendix B and C for a more formal definitions.

Topological data analysis is a data analysis tool based on algebraic topology. Topology studies shape (e.g., how many holes a configuration have) while algebra studies arithmetic (what are properties of a symbolic set under certain operational rules). Algebraic topology is a mathematical framework that studies the topological space using algebraic methods. This is partly possible because, from the view of topology, certain objects are "the same", or more precisely, equivalent, up to a special type of transformation called homeomorphism. Intuitively, it is a deformation, or stretching without breaking, e.g., see the figure below for a simple illustration in 1-dimension.

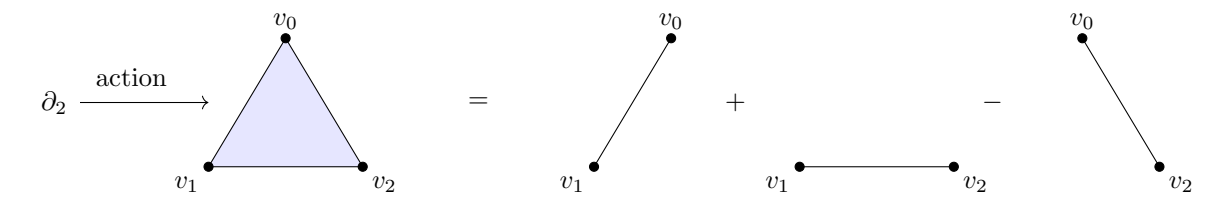


The above example features the fact that a curve, no matter how its shape look like, is equivalent to a straight line. The higher dimensional analog of this example can be carried out in a straightforward way. In 2-dimensional case, for instance, it can be seen that any surface domain is equivalent to a triangle. Thus, by reducing the seemingly complicated configuration to simpler ones, one can hope to gain its topological information easier.

These objects, including line, triangle, and higher-dimensional one, are the building blocks of algebraic topology, which are named simplexes. Figure 1 illustrates 0-simplex, 1-simplex, 2-simplex and 3-simplex. Higher-dimensional simplexes are built in a similar way: an r-simplex contains (r+1) geometrically independent points. A simplicial complex is built by gluing simplexes so that the intersection between arbitrary two simplexes is either another simplex or empty. Earlier, we have mentioned the notion of homeomorphism. If there is a homeomorphism between a topological space \mathcal{X} and a simplicial complex K, then K is called a triangulation of \mathcal{X} . The key philosophy of algebraic topology is that, by associating/approximating a continuous object (e.g., topological space) with discrete objects (simplicial complex – essentially a collection of simplexes), there exists a correspondence between their topological feature of the

former and algebraic feature of the latter. By analyzing the algebraic structure of the discrete representation, the topological feature of the original space can be inferred.

To analyze such an algebraic structure, it is necessary to assign certain algebraic properties to the given complex. Throughout our work, we use S_r to denote the set of r-simplexes in the complex K of interest. Then a (formally) linear combination of these r-simplexes form a r-chain. The collection of these chains thus form a r-chain group/space C_r . In particular, there is an important operation called boundary operator. Roughly speaking, it decomposes a simplex into a (formal) sum of its boundary. For instance, the boundary operator acts on 2-simplex as follows.



where the plus (+) or minus (-) sign depends on the order of the vertex removed. The generalization to higher-dimensional simplexes is straightforward, obeying the following formula:

$$\partial_r[p_0, p_1, \dots, p_r] = \sum_{i=0}^r (-1)^i [p_0, p_1, \dots, \hat{p_i}, \dots, p_r],$$
(1)

The action of the boundary operator ∂_r in the r-chain (linear combination of r-simplexes) is enacted by linearity. While a more detailed treatment of algebraic topology can be found in [27] (see also Appendix C), we remark that, as a fundamental result in algebraic topology, the topological structure of the given complex is encoded in the algebraic structure of the boundary operators. Specifically, suppose that we work over real field \mathbb{R} , then ∂_r becomes a linear map, and we have that the r-th homology space is defined as

$$H_r \equiv \text{Ker}(\partial_r)/\text{Im}(\partial_{r+1})$$
 (2)

The so-called r-th Betti number β_r is defined as:

$$\beta_r = \dim H_r = \dim \operatorname{Ker} (\Delta_r) \tag{3}$$

The operator $\Delta_r = \partial_{r+1} \partial_{r+1}^{\dagger} + \partial_r^{\dagger} \partial_r$ is named combinatorial Laplacian operator. Intuitively, β_r captures the number of r-dimensional holes in the complex. Thus, as we mentioned earlier, by algebraically analyzing the boundary operators, we can deduce the topological space, e.g., revealing how many holes it has.

To see how algebraic topology can be relevant to data analysis, we point out that, in reality, data usually come as vectors, or points in the Euclidean space, with mutual connectivity provided, e.g., a graph network, triangulated mesh, etc. Such a network can be treated as a simplicial complex, and thus, algebraic topology can be applied. In reality, there can be many data points, and they can be very high-dimensional. Thus, it presents a nontrivial challenge for analysis. For example, provided a dataset, a question one may ask is: how does the dataset look like? We have pointed out from the beginning that topology cares about shape, and thus, TDA emerges as a suitable tool for answering this question. Indeed, there have been many efforts to apply TDA [28–33]. These applications span many areas, from biomedicine, computer vision, to financial analysis. Their successes have affirmed that TDA is a powerful data analytical tool, and that it can complement nicely to the well-known ones, such as machine learning, statistical methods, etc.

III. A SURVEY OF QUANTUM TOPOLOGICAL DATA ANALYSIS

Quantum algorithms for topological data analysis (briefly called quantum TDA), specifically estimating Betti numbers, began with the work in [18], a.k.a LGZ algorithm. Their algorithm contains the following key components as well as related assumptions.

1. Encoding simplexes into computational basis states. Let the simplicial complex of interest K having N data points, denoted as $v_0, v_1, v_2, ..., v_N$. Then a r-simplex $\sigma_r \in K$ is encoded into a N-qubit string of Hamming weight $r+1 \mid \sigma_r \rangle$ as follows: if $v_i \in \sigma_r$ then the value of i-th bit is 1; otherwise, it is 0.

2. Oracle for verifying simplexes. For any r $(1 \le r \le N)$, there is an oracle O_r that acts as follows:

$$O_r |0\rangle |\sigma_r\rangle = \begin{cases} |1\rangle |\sigma_r\rangle & \text{if } s_r \in K \\ |0\rangle |\sigma_r\rangle & \text{otherwise} \end{cases}$$
 (4)

3. Entry-computability of boundary operators $\{\partial_r\}_{r=1}^N$. There are specifically two oracles. The first one computes the location of nonzero entries (for a given row/column). The second one computes the value of those entries. This assumption is essentially analogous to those appeared the context of Hamiltonian simulation [10–13]. In fact, the LGZ algorithm uses these quantum simulation algorithms as a subroutine.

With the above inputs, LGZ algorithm combines several well-known ones, including Grover's search algorithm (multi-solution version), quantum simulation, and quantum phase estimation, to construct a quantum procedure that estimates the r-th normalized Betti number $\frac{\beta_r}{|S_r|}$ (where we remind that S_r is the set of r-simplexes in K), up to some additive accuracy.

The LGZ algorithm has ignited many subsequent attempts, toward many directions. The work in [20] proposed to replace the Grover's search subroutine within LGZ algorithm by a method called rejection sampling. In addition, they also proposed replacing the quantum phase estimation subroutine with the stochastic rank estimation method, which was first introduced in [34, 35]. These two replacements resulted in a certain improvement over the LGZ algorithm, and as claimed in [20], it is very suitable for near-term era. Recent work [19] provides an in-depth analysis of quantum advantage in estimating Betti numbers. In particular, they introduced new ways to replace Grover's search algorithm (with Dicke state preparation) and amplitude estimation (using Kaiser window). They also provided specific type of graphs/complexes for which exponential quantum speedup is possible.

In addition to the two above, the work in [21, 22] also features another progress. Instead of estimating Betti numbers (as in [18–20]), the authors in [21, 22] focus on persistent Betti numbers and develop the corresponding quantum algorithms. We remind the reader that the Betti numbers capture the number of holes in a given complex. Persistent Betti numbers, on the other hand, capture the number of holes that survive over different *filtration*. To get more insight about filtration, one can imagine that a simplicial complex is built on simplexes, which are again built on data points and pairwise connectivity. Filtration roughly means denser and denser connectivity.

Aside from the algorithmic aspect, quantum TDA is also attracting attention from the complexity aspect. In particular, the work in [23] has shown that, provided pairwise connectivity, computing Betti numbers is #P-hard, while estimating them is NP-hard. A similar result obtained in [24], showing that estimating Betti numbers QMA-hard, while exactly computing them is BQP-hard. These results have implied a strong barrier on the potential of quantum exponential advantage in TDA. However, the work [36] has shown that the problem of estimating normalized Betti numbers is classically hard, which leaves a certain hope for quantum TDA. In fact, recent efforts [25, 26, 37] have shown that in structured settings, e.g., triangulated manifold [26], mutual relation between a pair of simplexes [25], or a graph with bounded degree [37], quantum computers can still offer a significant advantage.

IV. OUR CONTRIBUTION

The aforementioned works have featured a significant amount of interest in quantum TDA. Here, we make a relevant, yet fundamentally different progress toward this exciting direction. Instead of seeking the Betti numbers of a given complex, we are curious about the *torsion* of such the complex. To elaborate on this concept, we recall that earlier we mentioned that a r-chain is formed by taking a (formal) linear combination of r-simplexes. The collection of these chains form the r-chain group/space C_r . If the coefficients of the linear combination are drawn from real field \mathbb{R} , then C_r behaves as a linear vector space, for which the Betti numbers β_r can be estimated by probing the spectrum of corresponding Laplacian operators. In particular, we remark that all the works mentioned in the previous section are based on homology $over \mathbb{R}$ (see also Appendix \mathbb{C}). If instead of \mathbb{R} , the coefficients are drawn from the integer \mathbb{Z} , which is a ring, then it leads to a distinct separation.

First, over \mathbb{Z} , C_r is no longer a vector space. Rather, it is an Abelian group (or \mathbb{Z} -module). Second, because of this, ∂_r is no longer a linear mapping between vector spaces. Third, as a result, H_r is no longer a space but an Abelian group. Since it is an Abelian group, there exists a fundamental result in algebra (see Theorem 2 in the Appendix B), showing that H_r can be decomposed as:

$$H_r \cong \mathbb{Z}^{\beta_r} \oplus \left(\bigoplus_i Z_{r_i}\right) \tag{5}$$

where $r_i \mid r_{i+1}$ refers to the divisibility relation. We refer the readers to Appendix B for more a formal review of abstract algebra. The first part \mathbb{Z}^{β_r} is called *free part*, while the second part $(\bigoplus_i Z_{r_i})$ is *torsion part*. To this end, we have sufficient information to state the key objective of our work, which is:

Given a simplicial complex K, does it have torsion?

We remark a few things. In the setting \mathbb{Z} , H_r is no longer a vector space and, therefore, the notion of dim H_r is no longer relevant. Rather, it is rank H_r that is of interest. However, quantum computation is built on quantum mechanics, which is naturally built on the complex field \mathbb{C} . Thus, it is of fundamental constraint that prevents existing quantum algorithms from handling the torsion part appearing in the above formula.

Our solution to the above question and the corresponding quantum algorithm rely on a few insights. In the following, we attempt to summarize the main recipes and key steps. The detailed treatment shall be provided in the Appendix D, Appendix F and Appendix G.

A. Mathematical insight

Let $H_r(Q)$ to denote the r-th homology group H_r defined over Q, which can be a field (like real field \mathbb{R} , complex field \mathbb{C}) or a ring (like \mathbb{Z}). The first recipe we use is the well-known result within algebra, called *universal coefficient theorem*, which shows how the change in the choice of coefficients induces the change in the algebraic structure of the homology group:

$$H_r(Q) \cong H_r(\mathbb{Z}) \otimes_{\mathbb{Z}} Q \oplus \text{Tor}(H_{r-1}(\mathbb{Z}), Q)$$
 (6)

where the last term $\text{Tor}(H_{r-1}(\mathbb{Z}), \mathbb{R})$ is the torsion product functor (see further Appendix D for more details). If we choose $Q = \mathbb{F}_p \equiv \mathbb{Z}/p\mathbb{Z}$ for prime p, then we can turn \mathbb{F}_p into a field, i.e., it is a finite field. As it is a field, the chain group C_r becomes a vector space, and thus the homology group $H_r(\mathbb{F}_p)$ becomes a vector space. In the Appendix D and \mathbb{F} , using the above universal coefficient theorem and related properties of torsion product functor, we will prove the following:

$$\dim\left(H_{\mathbf{r}}(\mathbb{F}_{\mathbf{p}})\right) = \beta_{\mathbf{r}} + t_{\mathbf{r}} + t_{\mathbf{r}-1} \tag{7}$$

where t_r, t_{r-1} is the total amount of the cyclic summands (of k-th homology group/space and (k-1)-th homology group/space, respectively) of order divisible by a prime p. At the same time, if we choose $Q = \mathbb{R}$ as usual, then $H_r(\mathbb{R}) \cong \mathbb{Z}^{\beta_r}$ and thus dim $H_r(\mathbb{R}) = \beta_r$, which is exactly the r-th Betti number. Thus, our strategy is, we estimate the dimension of the homology group over \mathbb{R} , and \mathbb{F}_p for various values of prime p. If they are the same, then it implies that there is no torsion at the order r and r-1. Otherwise, there is. We remark a property that over finite field \mathbb{F}_p , it still holds that the dimension of homology group is equal to the dimension of the kernel of combinatorial Laplacian. However, we need to take into account the finite field, which results in that all arithmetic operations need to be done modulo p, e.g.,

$$\dim H_r(\mathbb{F}_p) = \dim \operatorname{Ker} \left(\Delta_{\mathbf{r}}\right)^{\operatorname{mod p}} \tag{8}$$

B. Necessary Recipes

Before we outline our algorithm, we remark that a majority of our work relies on block-encoding. We refer the unfamiliar readers to the Appendix A for a summary of formal definition as well as related operations involving block-encoding.

We first describe the input model on which we shall work. Some existing works, such as [18–20, 22, 23] assume an oracle that can verify the existence/non-existence of simplexes within the complex of interest. Particularly, the work [19] provides an explicit construction of such oracle, given the graph description of the interested complex. We name this setup oracle model. At the same time, recent results [25, 26] do not assume the oracle, and thus we name it non-oracle model. Rather, the input assumption is the classical knowledge/description of a matrix that encodes the mutual relation among simplexes. More specifically, let $S_r = \{\sigma_{r_1}, \sigma_{r_2}, ...\}$ denotes the set of r-simplexes in the complex of interest K. For some r, let \mathcal{D}_r denotes the matrix of size $|S_{r-1}| \times |S_r|$, which encodes the structure of the given complex as follows. For a given column index, say j (with $1 \le j \le |S_r|$), we have:

$$(\mathscr{D}_r)_{ij} = \begin{cases} 1 & \text{if } \sigma_{r_i} \cap \sigma_{(r-1)_j} \neq \emptyset \\ 0 & \text{if } \sigma_{r_i} \cap \sigma_{(r-1)_j} = \emptyset \end{cases}$$

$$(9)$$

The assumption is that for any r, the entries of \mathcal{D}_r are classically known/provided. As discussed in [25], a way to achieve this assumption is by direct specification, which is also partially suggested in [23]. In the Appendix G, we will describe this input model in greater detail, including an example for illustration. In the following, we proceed to describe our algorithm with the non-oracle model as input. Subsequently, we will show how the oracle model can also be easily integrated into our procedure.

To proceed, we point out the following result regarding state preparation with elements drawn from a finite field, which is an important recipe for our subsequent construction:

Lemma 1 (Finite-field state preparation [38–40])– Appendix J3). Given a N-dimensional quantum state $|\Phi\rangle = \frac{1}{||x||} \sum_{i=1}^{N} x_i |i\rangle$ where $||x|| = \sqrt{\sum_{i=1}^{N} x_i^2}$, and each x_i is drawn from a finite field, e.g., \mathbb{F}_p . Then there is a quantum procedure that prepares $|\Phi\rangle$, with circuit complexity $\mathcal{O}(\log N)$ and extra $\mathcal{O}(1)$ ancilla qubits.

Generally speaking, the above quantum procedure directly applies the state preparation protocols in [38-40]. For instance, according to Theorem 1 in [39], there is an efficient procedure to prepare the state of the form $|\Phi_f\rangle \sim \sum_{i=-\frac{N}{2}}^{\frac{N}{2}-1} f\left(\frac{2ai}{N}\right)|i\rangle$ (where \sim hides the normalization factor), where $f:[-a,a] \longrightarrow \mathbb{R}$ being some preferably smooth function (albeit a non-smooth function also works, as discussed in [39]). By choosing any f that satisfies $f(\frac{2ai}{N}) = x_i$, then the desired state $|\Phi\rangle$ can be prepared. The circuit complexity of this method is $\mathcal{O}(\log N)$, and at most 3 ancilla qubits. As a comment, in principle, any function f with values as desired can be used. In Appendix J3, we will describe an effective approach to obtain the desired f in practice. The general idea is to promote these amplitudes $\{x_i\}_{i=1}^N$ to the corresponding data points $\{(2ai/N,x_i)\}_{i=1}^N \in \mathbb{R}^2$. By connecting two consecutive data points (with respect to the index i), a piecewise-linear function is formed. Then we can apply existing methods [41-44] to find a good approximation, or even an exact function f with the properties as desired. Finally, in the same appendix, we will also discuss other means to prepare the state $|\Phi\rangle$ above, based on [38, 40], which also achieve the same complexity $\mathcal{O}(\log N)$.

As the next recipe, given the classical description of $\{\mathcal{D}_r\}$ as above, we have the following lemma, which is crucial to our subsequent construction:

Lemma 2 (Block-encoding of boundary operator – Appendix J). Provided the classical knowledge of \mathscr{D}_r described above, then there is a quantum procedure, using a $\mathcal{O}(\log(|\mathcal{S}_{r-1}||\mathcal{S}_r|))$ -qubits quantum circuit of depth $\mathcal{O}(\log(|\mathcal{S}_{r-1}||\mathcal{S}_r|))$ that produces an exact block-encoding of $\frac{\partial_r^{\dagger}\partial_r}{|\mathcal{S}_{r-1}||\mathcal{S}_r|}$, extra $\mathcal{O}(1)$ ancilla qubit, with further $\mathcal{O}(1)$ classical pre-processing.

This result is originally of [25] (which is based on [45]). To provide an overview of key ideas and steps, we note that the classical description of \mathcal{D}_r is translated into the classical description of ∂_r (almost by definition). Given such classical knowledge, using the state preparation algorithm [38–40], we can prepare the state that contains $\sim \sum_i \partial_r^i |i\rangle$ (where ∂_r^i is the *i*-th column of ∂_r , and \sim hides some scaling factor) as a sub-vector. From such the state, a few arithmetic recipes from block-encoding framework [46] (e.g., Lemma 6, Lemma 15 in the Appendix A) can be applied, resulting in the block-encoding of $\frac{\partial_r^i \partial_r}{|\mathcal{S}_{r-1}||\mathcal{S}_r|}$. Interested readers can find more details in our Appendix J, where we directly quote and discuss the proof from [25] in detail.

C. Quantum Algorithm

We use a classical random sampler to draw independent and identically distributed (i.i.d.) elements from \mathbb{F}_p . We then form $s \cdot t$ (for $s, t \in \mathbb{Z}_+$) vectors $u_1, u_2, ..., u_s, v_1, v_2, ..., v_t \in \mathbb{F}_p^{|\mathcal{S}_r|}$ with randomly i.i.d. entries drawn from \mathbb{F}_p . Then we use Lemma 1 to prepare the following states $|v_1\rangle, |v_2\rangle, ..., |v_t\rangle, |u_1\rangle, |u_2\rangle, ..., |u_s\rangle$. The value of $s, t \in \mathbb{Z}_+$ is chosen to guarantee a high success probability, as we will see below.

The reason why we need to prepare the above states with i.i.d. entries is for the purpose of finding the dimension of the rank of Δ_r (modulo p), which contains the dimension of the homology group of interest $H_r(\mathbb{F}_p)$. Existing quantum algorithms for finding kernel/rank employed in previous works can only handle real or complex field. In the finite field, these methods are no longer guaranteed to produce the correct solution as the arithmetic operation needs to be done modulo p. In order to handle the mod p operation, we rely on the classical algorithm introduced in [47, 48]. A summary of such algorithms can be found in Algorithm 4 in the Appendix I.

To proceed, via Lemma 2, we obtain the block-encoding U_r, U_{r+1} of $\frac{\partial_r^{\dagger} \partial_r}{|\mathcal{S}_{r-1}||\mathcal{S}_r|}$ and of $\frac{\partial_{r+1} \partial_{r+1}^{\dagger}}{|\mathcal{S}_r||\mathcal{S}_{r+1}|}$, respectively. Next, we use the Hadamard/SWAP test with advanced amplitude estimation [49–51] to estimate the overlaps

$$\langle \mathbf{0} | \langle u_i | U_r | \mathbf{0} \rangle | u_i \rangle$$
, $\langle \mathbf{0} | \langle u_i | U_{r+1} | \mathbf{0} \rangle | u_i \rangle$

up to a chosen additive precision ϵ . In particular, as will be shown in the appendix (see Lemma 12), the above inner product is equivalent to

$$\frac{u_{i}^{\dagger}\partial_{r}^{\dagger}\partial_{r}v_{j}}{||u_{i}||\ ||v_{j}|||\mathcal{S}_{r}||\mathcal{S}_{r-1}|}, \frac{u_{i}^{\dagger}\partial_{r+1}\partial_{r+1}^{\dagger}v_{j}}{||u_{i}||\ ||v_{j}|||\mathcal{S}_{r}||\mathcal{S}_{r+1}|}$$

In particular, by choosing

$$\epsilon = \frac{\eta |u_i^{\dagger} \partial_r^{\dagger} \partial_r v_j|}{||u_i|| \ ||v_i|| |\mathcal{S}_r||\mathcal{S}_{r-1}|}$$

then we can estimate $u_i^{\dagger} \partial_r^{\dagger} \partial_r v_j$, $u_i^{\dagger} \partial_{r+1} \partial_{r+1}^{\dagger} v_j$ and thus, $u_i^{\dagger} \Delta_r v_j$ to a multiplicative accuracy δ . As $u_i^{\dagger} \Delta_r v_j$ is ideally an integer, $\eta = 1/2$ suffices to infer the exact estimation, as we simply need to round $u_i^{\dagger} \Delta_r v_j$ to the nearest integer. We then build the matrix M of size $s \times t$ with the entries defined as follows

$$M_{ij} = u_i^{\dagger} \Delta_r v_j \tag{10}$$

Next, we need to take the modulo p of the above values, to obtain $M_{ij} \pmod{p}$. We then use the classical algorithm in [47, 48] (see algo Algo. 4) to find the rank of $M \pmod{p}$. Denote such rank as \hat{r}_p as the rank of $M \pmod{p}$. As proved in [47, 48], by choosing $s, t = \mathcal{O}\left(\log_p \frac{1}{\delta}\right)$, the value \hat{r}_p produces the exact rank of Δ_r with success probability $1 - \delta$.

The last step is straightforward. In order to detect the torsion, we repeat the above algorithm for a few values of p, and possibly over real field \mathbb{R} . Then we obtain a sequence of values $\{\hat{r}_{p_i}\}$ with $\{p_i\}$ being primes. By comparing them, the torsion can be detected.

Earlier, we have mentioned that the oracle model can be integrated into our algorithm simply. Here, we elaborate on this. Within the non-oracle model, the classical knowledge/description of the matrices $\{\mathscr{D}_r\}$ allow us to obtain the block-encoding of $\propto \partial_r^{\dagger} \partial_r$, $\partial_{r+1} \partial_{r+1}^{\dagger}$ (where \propto hides the appropriate scaling factor). Within the oracle model, it turns out that these operators can also be block-encoded via the result of [22] (see their Section 6). From such a block-encoding, we can proceed our algorithm outlined above, and thus being able to detect torsion eventually.

A detailed analysis on the complexity of our algorithm, in both oracle and non-oracle is provided in the Appendix H. We summarize our main result in the following:

Theorem 1 (Torsion Detection). Let K be the simplicial complex of interest, having N data points. Then:

• (Non-oracle regime) Provided the classical description of K via the matrices $\{\mathscr{D}_r\}_{r=1}^N$ as above, there is an algorithm that detects if K has torsion (at order r, or of r-th homology group) with a failure probability δ . For $S_r^{\max} = \max\{\mathcal{S}_{r-1}^K, \mathcal{S}_r^K, \mathcal{S}_{r+1}^K\}$, the algorithm has quantum complexity (quantum circuit complexity + total number of iterations)

$$\mathcal{O}\left(\log\left(S_r^{\max}\right)\frac{1}{\eta}S_r^{\max}\log_p^2\frac{1}{\delta}\right)$$

and employ a classical procedure of complexity $\mathcal{O}\left(\log\left(|\mathcal{S}_{r-1}||\mathcal{S}_r||\mathcal{S}_{r+1}|\right) + \log_p^2 \frac{1}{\delta}\right)$.

• (Oracle-regime) Provided the oracle O_r which can verify the inclusion of r-simplexes as above, there is an algorithm that detects if K has torsion at order r, or of r-th homology group) with a failure probability. The algorithm quantum complexity (quantum circuit depth + total number of iterations)

$$\mathcal{O}\left((N^2 + \log |\mathcal{S}_r|)N\frac{1}{\eta}\log_p^2\frac{1}{\delta}\right)$$

and employs a classical procedure of complexity $\mathcal{O}\left(\log\left(|\mathcal{S}_{r-1}||\mathcal{S}_r||\mathcal{S}_{r+1}|\right)\log^2\frac{1}{\delta}\right)$.

Potential advantage. To compare, we point out that the classical algorithm for detecting torsion can still rely on examining the behavior of homology groups H_r over different fields. A naive way is to compute the dimension of kernel of Δ_r directly, e.g., via exact diagonalization or Gaussian elimination. For a complex having $|\mathcal{S}_r|$ r-simplexes, we first need to build the boundary operators ∂_r , then building the Laplacian Δ_r , resulting in total complexity $\mathcal{O}(|\mathcal{S}_r|^{\omega})$ where ω is the matrix multiplication factor. Then applying diagonalization or Gaussian elimination incurs a total complexity $\mathcal{O}(|\mathcal{S}_r|^3)$. Alternatively, we can use the classical algorithm developed [47, 48] (see Algo. 4). Instead of diagonalizing Δ_r , we perform a sequence of matrix-vector products $v_j^{\dagger}\Delta_r u_i$ for $i=1,2,...,s,\ j=1,2,...,t$. Then we

build a matrix M of size $s \times t$ with $M_{ij} = v_j^{\dagger} \Delta_r u_i$. The rank, and thus, the kernel of Δ_r can be found by finding the rank of M, which can be done using exact diagonalization or Gaussian elimination. This approach will reduce the time complexity to $\mathcal{O}\left(|\mathcal{S}_r|^{\omega} + \log_p^2 \frac{1}{\delta}\right)$, with a success probability $1 - \delta$ for $s, t = \mathcal{O}\left(\log \frac{1}{\delta}\right)$. As indicated in the Theorem 1, quantum algorithm can offer an exponential speed-up with respect to the number of r-simplexes $|\mathcal{S}_r|$.

Comparing the classical complexity and our complexity in Theorem 1, it can be seen that in the non-oracle regime, there is almost a power-of-3 speed-up in $|\mathcal{S}_r|$. In the oracle-regime, if $N \ll \mathcal{S}_r$, e.g., when r is sufficiently large and the number of complexes \mathcal{S}_r is large (clique-dense), then there is an exponential speed-up in $|\mathcal{S}_r|$. On other hand, when $N \sim |\mathcal{S}_r|$, then there is no speedup.

V. DISCUSSION & CONCLUSION

In this work, we have proposed and analyzed a quantum algorithm for detecting torsion. Starting from the mathematical properties, specifically the algebraic structure of the homology groups, we outline a strategy for revealing the torsion from the complex. Our quantum algorithm is built upon severally recent advances in quantum algorithms, including [25, 45, 46], and the classical probabilistic method for rank estimation [47, 48]. As been analyzed, with a certain assist from classical computers and probabilistic guarantee, our quantum algorithm can provide a significant speed-up compared to the classical counterpart.

As mentioned in the introduction, the potential of quantum computation in TDA has been somewhat limited by the complexity-theoretic result of [23]. However, the result of this work has revealed that a fundamentally related problem can still be beneficial with quantum computers. Our work has suggested that there should be more room and opportunities for exploring quantum advantage in TDA, beyond the issue of Betti numbers. Below, we list several prospects that we think it is of high value.

- Our work has provided a quantum algorithm for detecting torsion. However, the structure of torsion can be complicated, e.g., of the form $\bigoplus_i Z_{r_i}$, and our algorithm cannot determine these factors $\{r_i\}$. The classical approach is to compute the Smith normal form for the boundary, or Laplacian operator. However, this approach is very computationally expensive. A direct translation of this procedure to quantum setting is not known to us. Even if there is, we suspect that the cost is high. Therefore, developing an efficient quantum algorithm for finding these invariant factors is of great interest.
- TDA has been proposed for a while, and the corresponding algorithms have been applied in many contexts. However, from a complexity-theoretic viewpoint, it just has been recently established [23, 24] that Betti numbers are difficult to estimate, and it is even harder to compute them exactly. Whether if there exists an analogous result regarding the torsion and its structure, specifically the invariant factors $\{r_i\}$, is unclear to us.

We believe that all these questions can foster new development toward quantum topological data analysis. We conclude our work here and leave them for future investigation.

ACKNOWLEDGEMENTS

Part of this work is done when the author is an intern at QuEra Computing Inc. We particularly acknowledge the hospitality of Harvard University where the author has an academic visit during the completion of this project.

^[1] Peter W Shor. Polynomial-time algorithms for prime factorization and discrete logarithms on a quantum computer. SIAM Review, 41(2):303–332, 1999.

^[2] Lov K Grover. A fast quantum mechanical algorithm for database search. In Proceedings of the twenty-eighth annual ACM Symposium on Theory of Computing, pages 212–219, 1996.

^[3] David Deutsch. Quantum theory, the church-turing principle and the universal quantum computer. Proceedings of the Royal Society of London. A. Mathematical and Physical Sciences, 400(1818):97–117, 1985.

^[4] David Deutsch and Richard Jozsa. Rapid solution of problems by quantum computation. *Proceedings of the Royal Society of London. Series A: Mathematical and Physical Sciences*, 439(1907):553–558, 1992.

^[5] Aram W Harrow, Avinatan Hassidim, and Seth Lloyd. Quantum algorithm for linear systems of equations. *Physical Review Letters*, 103(15):150502, 2009.

^[6] Dorit Aharonov and Amnon Ta-Shma. Adiabatic quantum state generation and statistical zero knowledge. In *Proceedings* of the thirty-fifth annual ACM symposium on Theory of computing, pages 20–29, 2003.

- [7] Seth Lloyd. Universal quantum simulators. Science, 273(5278):1073-1078, 1996.
- [8] Seth Lloyd, Masoud Mohseni, and Patrick Rebentrost. Quantum algorithms for supervised and unsupervised machine learning. arXiv preprint arXiv:1307.0411, 2013.
- [9] Seth Lloyd, Maria Schuld, Aroosa Ijaz, Josh Izaac, and Nathan Killoran. Quantum embeddings for machine learning. arXiv preprint arXiv:2001.03622, 2020.
- [10] Dominic W Berry, Graeme Ahokas, Richard Cleve, and Barry C Sanders. Efficient quantum algorithms for simulating sparse hamiltonians. *Communications in Mathematical Physics*, 270(2):359–371, 2007.
- [11] Dominic W Berry and Andrew M Childs. Black-box hamiltonian simulation and unitary implementation. Quantum Information and Computation, 12:29–62, 2009.
- [12] Dominic W Berry. High-order quantum algorithm for solving linear differential equations. *Journal of Physics A: Mathematical and Theoretical*, 47(10):105301, 2014.
- [13] Dominic W Berry, Andrew M Childs, and Robin Kothari. Hamiltonian simulation with nearly optimal dependence on all parameters. In 2015 IEEE 56th Annual Symposium on Foundations of Computer Science, pages 792–809. IEEE, 2015.
- [14] Dominic W Berry, Andrew M Childs, Richard Cleve, Robin Kothari, and Rolando D Somma. Simulating hamiltonian dynamics with a truncated taylor series. *Physical Review Letters*, 114(9):090502, 2015.
- [15] Dominic W Berry, Andrew M Childs, Aaron Ostrander, and Guoming Wang. Quantum algorithm for linear differential equations with exponentially improved dependence on precision. Communications in Mathematical Physics, 356:1057–1081, 2017.
- [16] Andrew M Childs, Robin Kothari, and Rolando D Somma. Quantum algorithm for systems of linear equations with exponentially improved dependence on precision. SIAM Journal on Computing, 46(6):1920–1950, 2017.
- [17] Kosuke Mitarai, Makoto Negoro, Masahiro Kitagawa, and Keisuke Fujii. Quantum circuit learning. Physical Review A, 98(3):032309, 2018.
- [18] Seth Lloyd, Silvano Garnerone, and Paolo Zanardi. Quantum algorithms for topological and geometric analysis of data. *Nature communications*, 7(1):1–7, 2016.
- [19] Dominic W Berry, Yuan Su, Casper Gyurik, Robbie King, Joao Basso, Alexander Del Toro Barba, Abhishek Rajput, Nathan Wiebe, Vedran Dunjko, and Ryan Babbush. Analyzing prospects for quantum advantage in topological data analysis. PRX Quantum, 5(1):010319, 2024.
- [20] Shashanka Ubaru, Ismail Yunus Akhalwaya, Mark S Squillante, Kenneth L Clarkson, and Lior Horesh. Quantum topological data analysis with linear depth and exponential speedup. arXiv preprint arXiv:2108.02811, 2021.
- [21] Sam McArdle, András Gilyén, and Mario Berta. A streamlined quantum algorithm for topological data analysis with exponentially fewer qubits. arXiv preprint arXiv:2209.12887, 2022.
- [22] Ryu Hayakawa. Quantum algorithm for persistent betti numbers and topological data analysis. Quantum, 6:873, 2022.
- [23] Alexander Schmidhuber and Seth Lloyd. Complexity-theoretic limitations on quantum algorithms for topological data analysis. *PRX Quantum*, 4:040349, Dec 2023.
- [24] Marcos Crichigno and Tamara Kohler. Clique homology is qma 1-hard. Nature Communications, 15(1):9846, 2024.
- [25] Junseo Lee and Nhat A Nghiem. New aspects of quantum topological data analysis: Betti number estimation, and testing and tracking of homology and cohomology classes. arXiv preprint arXiv:2506.01432, 2025.
- [26] Nhat A Nghiem, Xianfeng David Gu, and Tzu-Chieh Wei. Quantum algorithm for estimating betti numbers using a cohomology approach. arXiv preprint arXiv:2309.10800, 2023.
- [27] Allen Hatcher. Algebraic topology. Cambridge University Press, 2005.
- [28] Gunnar Carlsson and Mikael Vejdemo-Johansson. Topological data analysis with applications. Cambridge University Press, 2021.
- [29] Anuraag Bukkuri, Noemi Andor, and Isabel K Darcy. Applications of topological data analysis in oncology. Frontiers in artificial intelligence, 4:659037, 2021.
- [30] Yashbir Singh, Colleen M Farrelly, Quincy A Hathaway, Tim Leiner, Jaidip Jagtap, Gunnar E Carlsson, and Bradley J Erickson. Topological data analysis in medical imaging: current state of the art. *Insights into Imaging*, 14(1):58, 2023.
- [31] Alice Patania, Francesco Vaccarino, and Giovanni Petri. Topological analysis of data. EPJ Data Science, 6(1):1–6, 2017.
- [32] Lee M Seversky, Shelby Davis, and Matthew Berger. On time-series topological data analysis: New data and opportunities. In *Proceedings of the IEEE conference on computer vision and pattern recognition workshops*, pages 59–67, 2016.
- [33] Peter Bubenik et al. Statistical topological data analysis using persistence landscapes. *Journal of Machine Learning Research*, 16(1):77–102, 2015.
- [34] Shashanka Ubaru and Yousef Saad. Fast methods for estimating the numerical rank of large matrices. In *International Conference on Machine Learning*, pages 468–477. PMLR, 2016.
- [35] Shashanka Ubaru, Yousef Saad, and Abd-Krim Seghouane. Fast estimation of approximate matrix ranks using spectral densities. *Neural Computation*, 29(5):1317–1351, 2017.
- [36] Casper Gyurik, Chris Cade, and Vedran Dunjko. Towards quantum advantage via topological data analysis. Quantum, 6:855, 2022.
- [37] Nhat A Nghiem, Junseo Lee, and Tzu-Chieh Wei. Hybrid quantum-classical framework for betti number estimation with applications to topological data analysis. arXiv preprint arXiv:2508.01516, 2025.
- [38] Gabriel Marin-Sanchez, Javier Gonzalez-Conde, and Mikel Sanz. Quantum algorithms for approximate function loading. *Physical Review Research*, 5(3):033114, 2023.
- [39] Sam McArdle, András Gilyén, and Mario Berta. Quantum state preparation without coherent arithmetic. arXiv preprint arXiv:2210.14892, 2022.

- [40] Kouhei Nakaji, Shumpei Uno, Yohichi Suzuki, Rudy Raymond, Tamiya Onodera, Tomoki Tanaka, Hiroyuki Tezuka, Naoki Mitsuda, and Naoki Yamamoto. Approximate amplitude encoding in shallow parameterized quantum circuits and its application to financial market indicators. *Physical Review Research*, 4(2):023136, 2022.
- [41] Yaron Lipman and David Levin. Approximating piecewise-smooth functions. *IMA journal of numerical analysis*, 30(4):1159–1183, 2010.
- [42] Victor M Jimenez-Fernandez, Maribel Jimenez-Fernandez, Hector Vazquez-Leal, Evodio Muñoz-Aguirre, Hector H Cerecedo-Nuñez, Uriel A Filobello-Niño, and Francisco J Castro-Gonzalez. Transforming the canonical piecewise-linear model into a smooth-piecewise representation. SpringerPlus, 5(1):1612, 2016.
- [43] Elmehdi Amhraoui and Tawfik Masrour. Smoothing approximations for piecewise smooth functions: A probabilistic approach. *Numerical Algebra, Control and Optimization*, 12(4):745–762, 2022.
- [44] Francesc Arandiga, Albert Cohen, Rosa Donat, and Nira Dyn. Interpolation and approximation of piecewise smooth functions. SIAM Journal on Numerical Analysis, 43(1):41–57, 2005.
- [45] Nhat A Nghiem. Refined quantum algorithms for principal component analysis and solving linear system. arXiv preprint arXiv:2504.00833, 2025.
- [46] András Gilyén, Yuan Su, Guang Hao Low, and Nathan Wiebe. Quantum singular value transformation and beyond: exponential improvements for quantum matrix arithmetics. In Proceedings of the 51st Annual ACM SIGACT Symposium on Theory of Computing, pages 193–204, 2019.
- [47] Erich Kaltofen and B David Saunders. On wiedemann's method of solving sparse linear systems. In *International Symposium on Applied Algebra, Algebraic Algorithms, and Error-Correcting Codes*, pages 29–38. Springer, 1991.
- [48] Wayne Eberly. Black box linear algebra: Extending wiedemann's analysis of a sparse matrix preconditioner for computations over small fields. ACM Communications in Computer Algebra, 50(4):164–166, 2017.
- [49] Patrick Rall. Faster coherent quantum algorithms for phase, energy, and amplitude estimation. Quantum, 5:566, 2021.
- [50] Patrick Rall and Bryce Fuller. Amplitude estimation from quantum signal processing. Quantum, 7:937, 2023.
- [51] Scott Aaronson and Patrick Rall. Quantum approximate counting, simplified. In Symposium on simplicity in algorithms, pages 24–32. SIAM, 2020.
- [52] Guang Hao Low and Isaac L Chuang. Optimal hamiltonian simulation by quantum signal processing. *Physical Review Letters*, 118(1):010501, 2017.
- [53] Guang Hao Low and Isaac L Chuang. Hamiltonian simulation by qubitization. Quantum, 3:163, 2019.
- [54] Daan Camps and Roel Van Beeumen. Approximate quantum circuit synthesis using block encodings. *Physical Review A*, 102(5):052411, 2020.
- [55] Joseph Gallian. Contemporary abstract algebra. Chapman and Hall/CRC, 2021.
- [56] Pierre Antoine Grillet. Abstract algebra. Springer, 2007.
- [57] Mikio Nakahara. Geometry, topology and physics. CRC press, 2018.
- [58] Jean-Guillaume Dumas and Clément Pernet. Computational linear algebra over finite fields. arXiv preprint arXiv:1204.3735, 2012.
- [59] Lov Grover and Terry Rudolph. Creating superpositions that correspond to efficiently integrable probability distributions. arXiv preprint quant-ph/0208112, 2002.

Appendix A: Block-encoding and quantum singular value transformation

We briefly summarize the essential quantum tools used in our algorithm. For conciseness, we highlight only the main results and omit technical details, which are thoroughly covered in [46]. An identical summary is also presented in [25].

Definition 1 (Block-encoding unitary, see e.g. [46, 52, 53]). Let A be a Hermitian matrix of size $N \times N$ with operator norm ||A|| < 1. A unitary matrix U is said to be an exact block encoding of A if

$$U = \begin{pmatrix} A & * \\ * & * \end{pmatrix},\tag{A1}$$

where the top-left block of U corresponds to A. Equivalently, one can write

$$U = |\mathbf{0}\rangle\langle\mathbf{0}| \otimes A + (\cdots), \tag{A2}$$

where $|\mathbf{0}\rangle$ denotes an ancillary state used for block encoding, and (\cdots) represents the remaining components orthogonal to $|\mathbf{0}\rangle\langle\mathbf{0}|\otimes A$. If instead U satisfies

$$U = |\mathbf{0}\rangle\langle\mathbf{0}| \otimes \tilde{A} + (\cdots), \tag{A3}$$

for some \tilde{A} such that $||\tilde{A} - A|| \leq \epsilon$, then U is called an ϵ -approximate block encoding of A. Furthermore, the action of U on a state $|\mathbf{0}\rangle |\phi\rangle$ is given by

$$U|\mathbf{0}\rangle|\phi\rangle = |\mathbf{0}\rangle A|\phi\rangle + |\text{garbage}\rangle,$$
 (A4)

where $|garbage\rangle$ is a state orthogonal to $|\mathbf{0}\rangle A |\phi\rangle$. The circuit complexity (e.g., depth) of U is referred to as the complexity of block encoding A.

Based on Definition 1, several properties, though immediate, are of particular importance and are listed below.

Remark 1 (Properties of block-encoding unitary). The block-encoding framework has the following immediate consequences:

- (i) Any unitary U is trivially an exact block encoding of itself.
- (ii) If U is a block encoding of A, then so is $\mathbb{I}_m \otimes U$ for any $m \geq 1$.
- (iii) The identity matrix \mathbb{I}_m can be trivially block encoded, for example, by $\sigma_z \otimes \mathbb{I}_m$.

Given a set of block-encoded operators, various arithmetic operations can be done with them. Here, we simply introduce some key operations that are especially relevant to our algorithm, focusing on how they are implemented and their time complexity, without going into proofs. For more detailed explanations, see [46, 54].

Lemma 3 (Informal, product of block-encoded operators, see e.g. [46]). Given unitary block encodings of two matrices A_1 and A_2 , with respective implementation complexities T_1 and T_2 , there exists an efficient procedure for constructing a unitary block encoding of the product A_1A_2 with complexity $T_1 + T_2$.

Lemma 4 (Informal, tensor product of block-encoded operators, see e.g. [54, Theorem 1]). Given unitary block-encodings $\{U_i\}_{i=1}^m$ of multiple operators $\{M_i\}_{i=1}^m$ (assumed to be exact), there exists a procedure that constructs a unitary block-encoding of $\bigotimes_{i=1}^m M_i$ using a single application of each U_i and $\mathcal{O}(1)$ SWAP gates.

Lemma 5 (Informal, linear combination of block-encoded operators, see e.g. [46, Theorem 52]). Given the unitary block encoding of multiple operators $\{A_i\}_{i=1}^m$. Then, there is a procedure that produces a unitary block encoding operator of $\sum_{i=1}^m \pm (A_i/m)$ in time complexity $\mathcal{O}(m)$, e.g., using the block encoding of each operator A_i a single time.

Lemma 6 (Informal, Scaling multiplication of block-encoded operators). Given a block encoding of some matrix A, as in Definition 1, the block encoding of A/p where p > 1 can be prepared with an extra $\mathcal{O}(1)$ cost.

Lemma 7 (Matrix inversion, see e.g. [16, 46]). Given a block encoding of some matrix A with operator norm $||A|| \le 1$ and block-encoding complexity T_A , then there is a quantum circuit producing an ϵ -approximated block encoding of A^{-1}/κ where κ is the conditional number of A. The complexity of this quantum circuit is $\mathcal{O}(\kappa T_A \log(1/\epsilon))$.

Lemma 8. [[46] Theorem 30] Let U, Π , $\widetilde{\Pi} \in \operatorname{End}(\mathcal{H}_U)$ be linear operators on \mathcal{H}_U such that U is a unitary, and Π , $\widetilde{\Pi}$ are orthogonal projectors. Let $\gamma > 1$ and $\delta, \epsilon \in (0, \frac{1}{2})$. Suppose that $\widetilde{\Pi}U\Pi = W\Sigma V^{\dagger} = \sum_i \varsigma_i |w_i\rangle \langle v_i|$ is a singular value decomposition. Then there is an $m = \mathcal{O}\left(\frac{\gamma}{\delta}\log\left(\frac{\gamma}{\epsilon}\right)\right)$ and an efficiently computable $\Phi \in \mathbb{R}^m$ such that

$$\left(\left\langle +\right| \otimes \widetilde{\Pi}_{\leq \frac{1-\delta}{\gamma}}\right) U_{\Phi}\left(\left|+\right\rangle \otimes \Pi_{\leq \frac{1-\delta}{\gamma}}\right) = \sum_{i: \ \varsigma_{i} \leq \frac{1-\delta}{\gamma}} \widetilde{\varsigma}_{i} \left|w_{i}\right\rangle \left\langle v_{i}\right|, \ \ where \ \left\|\frac{\widetilde{\varsigma}_{i}}{\gamma \varsigma_{i}} - 1\right\| \leq \epsilon. \tag{A5}$$

Moreover, U_{Φ} can be implemented using a single ancilla qubit with m uses of U and U^{\dagger} , m uses of $C_{\Pi}NOT$ and m uses of $C_{\widetilde{\Pi}}NOT$ gates and m single qubit gates. Here,

- $C_{\Pi}NOT:=X\otimes\Pi+I\otimes(I-\Pi)$ and a similar definition for $C_{\widetilde{\Pi}}NOT$; see Definition 2 in [46],
- U_{Φ} : alternating phase modulation sequence; see Definition 15 in [46],
- $\Pi_{\leq \delta}$, $\widetilde{\Pi}_{\leq \delta}$: singular value threshold projectors; see Definition 24 in [46].

Lemma 9. [[46] Theorem 56] Suppose that U is an (α, a, ϵ) -encoding of a Hermitian matrix A. (See Definition 43 of [46] for the definition.) If $P \in \mathbb{R}[x]$ is a degree-d polynomial satisfying that

• for all $x \in [-1,1]$: $|P(x)| \le \frac{1}{2}$,

then, there is a quantum circuit \tilde{U} , which is an $(1, a+2, 4d\sqrt{\frac{\varepsilon}{\alpha}})$ -encoding of $P(A/\alpha)$ and consists of d applications of U and U^{\dagger} gates, a single application of controlled-U and $\mathcal{O}((a+1)d)$ other one- and two-qubit gates.

Appendix B: Abstract Algebra

In this section, we provide an overview of algebra, showing essential concepts to understand the meaning of torsion. As a consequence, we aim to comprehend the role of coefficients and how it can affect the Betti numbers – a central problem within TDA, as mentioned in the main text. A more detailed introduction to abstract algebra can be found in standard textbook, e.g., [55, 56].

Definition 2 (Group). A group \mathcal{G} is a set equipped with an operation, denoted as *, with the following so-called group axioms:

- 1. Closure: if $a, b \in \mathcal{G}$ then $a * b \in X$.
- 2. **Associativity:** a * (b * c) = (a * b) * c.
- 3. **Identity:** There is a namely identity element e such that a * e = e * a = a.
- 4. Inverse: Every element a has an inverse element a^{-1} s.t. $aa^{-1} = a^{-1}a = e$.

A group is said to be Abelian if the group operation between two elements commute, i.e., for any $a, b \in \mathcal{G}$, we have that a * b = b * a. Abelian group is very common in many contexts, e.g., any vector space is an Abelian group.

Definition 3 (Torsion). Given an Abelian group \mathcal{G} , an element $x \in \mathcal{G}$ is a **torsion element** if there is some positive integer n that makes $x * x * x * \cdots * x$ (n times) an identity element e. If there is no such integer n exists, then x is called **free**.

Examples:

- In \mathbb{Z}_6 (integers mod 6), which we conveniently denote as $\{0,1,2,3,4,5\}$, then 2 is torsion element.
- In \mathbb{Z} , there is no torsion except 0 the identity element.

Given multiple groups, it is possible to "build" a larger group from these smaller groups while keeping their respective structure. The procedure is called *direct sum*.

Definition 4 (Direct Sum). If A and B are two groups, then their direct sum is:

$$A \oplus B = \{(a,b) \mid a \in A, b \in B\}$$
(B1)

with the component-wise operation is defined as:

$$(a_1, b_1) + (a_2, b_2) = (a_1 + a_2, b_1 + b_2)$$
(B2)

where $a_1, a_2 \in A, b_1, b_2 \in B$.

It can be seen that if A, B is Abelian, then $A \oplus B$ is Abelian. The above construction holds for more composing groups, that is, we can build "larger" groups, e.g., $A_1 \oplus A_2 \oplus A_3 \oplus \cdots \oplus A_n$.

Given a group \mathcal{G} , assumed to be Abelian for simplicity, with group operation *. Let $x \in \mathcal{G}$, $n \in \mathbb{Z}$ be some integers, and define $nx \equiv x * x * x * \cdots * x$ (n times). Then \mathcal{G} is said to be finitely generated if every element of \mathcal{G} can be expressed as $\sum n_i x_i$ where $n_i \in \mathbb{Z}$ and $x_i \in \mathcal{G}$. In this case, $\{x_i\}$ is said to be the generator of \mathcal{G} . We point out the following examples to illustrate this definition of generator:

- The Abelian group \mathbb{Z}^2 is generated by (1,0) and (0,1).
- The group $\mathbb{Z}_6 \equiv \{0, 1, 2, 3, 4, 5\}$ is generated by 1.

At the heart of abstract algebra is the following theorem, popularly known as the structured theorem:

Theorem 2 (Structured Theorem for Finitely Generated Abelian Groups). Every finitely generated Abelian group \mathcal{G} can be decomposed as:

$$\mathcal{G} \cong \mathbb{Z}^r \oplus \mathbb{Z}_{d_1} \oplus \mathbb{Z}_{d_2} \oplus \cdots \oplus \mathbb{Z}_{d_m} \tag{B3}$$

where:

- 1. r = rank, which is the number of independent "infinite" directions.
- 2. Each \mathbb{Z}_{d_i} is a finite cyclic group of size d_i .
- 3. It holds that $d_1|d_2|\cdots|d_m$ where $d_i|d_{i+1}$ denotes the divisibility.

The first part \mathbb{Z}^r is called free part and $\mathbb{Z}_{d_1} \oplus \mathbb{Z}_{d_2} \oplus \cdots \oplus \mathbb{Z}_{d_m}$ is called torsion part.

Aside from group, there are other algebraic objects, including ring and field.

Definition 5 (Ring). A ring R is a set equipped with two operations:

- 1. Addition (+), making (R,+) an Abelian group.
- 2. Multiplication (*), making (R,*) a semingroup with an associativity (a*b)*c = a*(b*c).
- 3. Distributivity: for all $a, b, c \in R$, it holds that:

$$a * (b+c) = a * b + a * c \tag{B4}$$

$$(a+b)*c = a*c + b*c$$
 (B5)

A ring might not have a multiplicative identity. If it does, denote the identity as 1_R (which is not the identity element of the Abelian group under (+) operation), then we call R a ring with unity. If the multiplicative operation commutes, for example, a*b=b*a, then the ring R is called a commute ring (possibly with unity).

Example: \mathbb{Z} (the integers) is a commutative ring with unity.

Definition 6 (Field). A field is a commutative ring R with unity, where it holds that every element has a multiplicative inverse, e.g., for any $a \in R$, there is another b such that $a * b = 1_R$.

Examples: $\mathbb{Q}, \mathbb{R}, \mathbb{C}$ are infinite fields. \mathbb{Z}_p with p prime is a field.

In the above, we have defined what it means to be a group and an Abelian group. It can be seen that a vector space is an Abelian group, with vector addition (+) as a group operation. A vector space is usually defined over some field \mathbb{F} , and a vector space is also equipped with a scalar multiplication (with a few axioms associated). A generalization of vector space is called a *module*, which is defined over a ring instead of a field.

Definition 7 (Module). Let R be some ring. An R-module M is:

- 1. An Abelian group (M, +).
- 2. Equipped with scalar multiplication $R \times M \longrightarrow M$, written $(r, m) \longrightarrow rm$ satisfying:
 - $r(m_1 + m_2) = rm_1 + rm_2$.
 - $(r_1 + r_2)m = r_1m + r_2m$.
 - $(r_1r_2)m = r_1(r_2m)$.
 - $1_R m = m$ (where 1_R denotes the identity element in the ring R).

We recall a basis of a vector space in which an arbitrary element of some space can be written as a linear combination of the elements in the basis. For a set S, the free module F(S) is made of (formal) linear combination of elements of S with coefficients from a ring R. In linear algebra, given two vector spaces, one can construct the tensor product of them. In the setting of module, two modules can be tensor producted. Yet, the rule is different.

Definition 8 (Tensor product of module). Given two R-modules M, N, the tensor product $M \otimes_R N$ is defined as:

$$M \otimes_R N = F/(bilinear\ relation)$$
 (B6)

where F is the free module generated by the pair (m,n) and the bilinear relation is:

- $(m_1 + m_2, n) = (m_1, n) + (m_2, n)$.
- $(m, n_1 + n_2) = (m, n_1) + (m, n_2).$
- (rm, n) = r(m, n) = (m, rn).

The following properties are imposed within tensor product:

- 1. $(m_1 + m_2) \otimes n = m_1 \otimes n + m_2 \otimes n$.
- 2. $m \otimes (n_1 + n_2) = m \otimes n_1 + m \otimes n_2$.
- 3. $(rm) \otimes n = m \otimes (rn)$.

It can be seen that any Abelian group \mathcal{G} , with group operation (*), is a \mathbb{Z} -module, by defining the action $nx = x * x * x * \cdots * x$ (n times) for $n \in \mathbb{Z}$ and $x \in \mathcal{G}$. We point out a few properties regarding computing tensor product between \mathbb{Z} -modules and other module:

Lemma 10 (Tensor product of \mathbb{Z} -modules). Let \mathbb{Z} be the set of integers. Then it holds that:

- $\mathbb{Z}^r \otimes_{\mathbb{Z}} N \cong N^r$ for arbitrary \mathbb{Z} -module N.
- $\mathbb{Z}_m \otimes_{\mathbb{Z}} \mathbb{Z}_n \cong \mathbb{Z}_{\gcd(m,n)}$.
- $\mathbb{Z}_m \otimes_{\mathbb{Z}} Q = 0$ for Q being a field of characteristic zero.
- $\mathbb{Z}^r \otimes_{\mathbb{Z}} Q \cong Q^r$

For illustration, we provide the following examples.

Example 1. Let $M = \mathbb{Z}^2 \oplus \mathbb{Z}_4$, and $N = \mathbb{Z}_6$ be \mathbb{Z} -modules. Then we have the following.

$$M \otimes_{\mathbb{Z}} N = (\mathbb{Z}^2 \oplus \mathbb{Z}_4) \otimes_{\mathbb{Z}} \mathbb{Z}_6 \tag{B7}$$

$$= (\mathbb{Z}^2 \otimes_{\mathbb{Z}} \mathbb{Z}_6) \oplus (\mathbb{Z}_4 \otimes_{\mathbb{Z}} \mathbb{Z}_6) \tag{B8}$$

$$=\mathbb{Z}_6^2 \oplus \mathbb{Z}_2 \tag{B9}$$

Example 2. Let $M = \mathbb{Z}^2 \oplus \mathbb{Z}_4$ and N = Q. Then we have:

$$M \otimes_{\mathbb{Z}} N = (\mathbb{Z}^2 \oplus \mathbb{Z}_4) \otimes_{\mathbb{Z}} Q \tag{B10}$$

$$= (\mathbb{Z}^2 \otimes_{\mathbb{Z}} Q) \oplus (\mathbb{Z}_4 \otimes_{\mathbb{Z}} Q) \tag{B11}$$

$$=0 (B12)$$

From the above example, we see that whenever a Z-module is tensor producted with a field (of characteristic zero), then the resulting module is zero. Subsequently, we will point out that this accounts for the fact that homology built on real coefficients miss the torsion part.

Appendix C: Algebraic Topology

This appendix provides a concise overview of the fundamental concepts in algebraic topology relevant to our work. We primarily follow the exposition of Nakahara [27, 57], to which we refer interested readers for comprehensive treatment of the subject.

Definition 9 (Simplex). Let $p_0, p_1, \ldots, p_r \in \mathbb{R}^m$ be geometrically independent points where $m \geq r$. The r-simplex $\sigma_r = [p_0, p_1, \ldots, p_r]$ is defined as:

$$\sigma_r = \left\{ x \in \mathbb{R}^m : x = \sum_{i=0}^r c_i p_i, \quad c_i \ge 0, \quad \sum_{i=0}^r c_i = 1 \right\},\tag{C1}$$

where the coefficients (c_0, c_1, \ldots, c_r) are called the barycentric coordinates of x.

Geometrically, a 0-simplex $[p_0]$ represents a point, a 1-simplex $[p_0, p_1]$ represents a line segment, a 2-simplex $[p_0, p_1, p_2]$ represents a triangle, and higher-dimensional simplices generalize this pattern to higher dimensions.

An r-simplex can be assigned an orientation. For instance, the 1-simplex $[p_0, p_1]$ has orientation $p_0 \to p_1$, which differs from $[p_1, p_0]$. Throughout this work, we adopt the convention that for an r-simplex $[p_0, p_1, \ldots, p_r]$, the indices are ordered from low to high, indicating the canonical orientation.

Definition 10 (Face and simplicial complex). For an r-simplex $[p_0, p_1, \ldots, p_r]$, any (s+1)-subset of its vertices defines an s-face σ_s where $s \leq r$. A simplicial complex K is a finite collection of simplices satisfying:

- 1. Every face of a simplex in K is also in K
- 2. The intersection of any two simplices in K is either empty or a common face of both simplices

The dimension of K is $\dim(K) = \max\{r : \sigma_r \in K\}$.

Definition 11 (Chain group). Let K be an n-dimensional simplicial complex. The r-th chain group C_r^K is the free abelian group generated by the oriented r-simplices of K. For $r > \dim(K)$, we define $C_r^K = 0$. Formally, let $S_r^K = \{\sigma_{r,1}, \sigma_{r,2}, \ldots, \sigma_{r,|S_r^K|}\}$ denote the set of r-simplices in K. An r-chain is an element of the form:

$$c_r = \sum_{i=1}^{|S_r^K|} c_i \sigma_{r,i} \tag{C2}$$

where $c_i \in \mathbb{R}$ are real coefficients. The group operation is defined by:

$$c_r^{(1)} + c_r^{(2)} = \sum_{i=1}^{|S_r^K|} \left(c_i^{(1)} + c_i^{(2)} \right) \sigma_{r,i}, \tag{C3}$$

making C_r^K a free abelian group of rank $|S_r^K|$.

In fact, since the coefficients $\{c_i\}$ belong to a field \mathbb{R} , the group C_r^K is also a vector space. In the following, we use the Abelian group/vector space interchangeably. The boundary operator $\partial_r: C_r^K \to C_{r-1}^K$ is fundamental to homological algebra.

Definition 12 (Boundary operator). For an r-simplex $[p_0, p_1, \ldots, p_r]$, the boundary operator is defined as:

$$\partial_r[p_0, p_1, \dots, p_r] = \sum_{i=0}^r (-1)^i [p_0, p_1, \dots, \hat{p_i}, \dots, p_r],$$
 (C4)

where $\hat{p_i}$ indicates that vertex p_i is omitted, yielding an (r-1)-simplex.

For an r-chain $c_r = \sum_{i=1}^{|S_r^K|} c_i \sigma_{r,i}$, we extend linearly:

$$\partial_r c_r = \sum_{i=1}^{|S_r^K|} c_i \partial_r \sigma_{r,i}.$$
 (C5)

The boundary operators form a chain complex:

$$0 \to C_n^K \xrightarrow{\partial_n} C_{n-1}^K \xrightarrow{\partial_{n-1}} \cdots \xrightarrow{\partial_1} C_0^K \xrightarrow{\partial_0} 0.$$
 (C6)

Definition 13 (Cycles, boundaries, and homology). An r-chain c_r is called an r-cycle if $\partial_r c_r = 0$. The collection of all r-cycles forms the r-cycle group $Z_r^K = \ker(\partial_r)$. Conversely, an r-chain c_r is called an r-boundary if there exists an (r+1)-chain d_{r+1} such that $\partial_{r+1}d_{r+1} = c_r$. The set of all r-boundaries forms the r-boundary group $B_r^K = \operatorname{im}(\partial_{r+1})$.

A fundamental property of boundary operators is that $\partial_r \circ \partial_{r+1} = 0$, which ensures that every boundary is also a cycle, i.e., $B_r^K \subseteq Z_r^K$. This inclusion allows us to define the r-th homology group/space as the quotient group/space $H_r^K = Z_r^K/B_r^K$, which captures the notion of cycles that are not boundaries.

Definition 14 (Betti numbers). The r-th Betti number is defined as:

$$\beta_r = \dim(H_r^K) = \dim(Z_r^K) - \dim(B_r^K). \tag{C7}$$

In the group-theoretic language, the above dimension, e.g., $\dim(H_r^K)$, is replaced by $\operatorname{rank}(H_r^K)$. As we mentioned, we use the notion of group/space interchangeably. For computational purposes, we can utilize the combinatorial Laplacian:

$$\Delta_r = \partial_{r+1} \partial_{r+1}^{\dagger} + \partial_r^{\dagger} \partial_r, \tag{C8}$$

where ∂_r^{\dagger} denotes the adjoint of ∂_r . A fundamental result in algebraic topology establishes that:

$$H_r^K \cong \ker(\Delta_r),$$
 (C9)

providing a direct method for computing Betti numbers via kernel dimension.

A central theorem in algebraic topology states that homology groups constitute topological invariants [27]:

Theorem 3 (Topological invariance of homology). If two topological spaces X and Y are homeomorphic, then their homology groups are isomorphic: $H_r^X \cong H_r^Y$ for all $r \geq 0$. Consequently, their Betti numbers are equal: $\beta_r^X = \beta_r^Y$.

This invariance property makes Betti numbers powerful tools for topological classification and forms the mathematical foundation for their applications in topological data analysis.

Appendix D: Role of Coefficients

In the above, we have built the chain group/space by taking (formal) linear combination of simplexes, with coefficients coming from a field. More concretely, we have defined the r-chain as:

$$c_r = \sum_{i=1}^{|S_r^K|} c_i \sigma_{r,i} \tag{D1}$$

where $\{c_i\} \in \mathbb{R}$. Instead, if we choose $\{c_i\}$ from the set of integers \mathbb{Z} , then the resulting set $C_r^K \equiv \{c_r = \sum_{i=1}^{|S_r^K|} c_i \sigma_{r,i}\}$ is not a vector space, but just an Abelian group. We emphasize the subtlety that a vector space is inherently an

Abelian group, but an Abelian group is not necessarily a vector space (as the multiplication by a scalar might not be properly defined, and also the scalar does not necessarily come from a field).

Changing the coefficients results in the change in the algebraic structure of homology groups. Suppose that we begin with the coefficients $\{c_i\} \in \mathbb{Z}$, then the k-th homology group $H_r(\mathbb{Z})$ is an Abelian group (where we specify \mathbb{Z} to explicitly imply the choice of coefficients from \mathbb{Z}). According to Theorem 2, $H_r(\mathbb{Z})$ admits the following decomposition:

$$H_r(\mathbb{Z}) \cong \operatorname{Free}(H_r(\mathbb{Z})) \oplus \operatorname{Torsion}(H_r(\mathbb{Z}))$$
 (D2)

where the free part Free generally has the form \mathbb{Z}^r in which r is called the rank, or the Betti numbers. The torsion part Tor is generally of the form $\mathbb{Z}_{d_1} \oplus \mathbb{Z}_{d_2} \oplus \cdots$ with the divisibility relation $d_i|d_{i+1}$. We can see that the Tor part is the main difference between homology with integer coefficients and real coefficients. To be more specific, if we change the choice of coefficients $\{c_i\}$ from \mathbb{Z} to \mathbb{R} , then there is a so-called universal coefficient theorem, which relates the change in the structure of homology group (under corresponding coefficients' type):

$$H_r(\mathbb{R}) \cong H_r(\mathbb{Z}) \otimes_{\mathbb{Z}} \mathbb{R} \oplus \text{Tor} (H_{r-1}(\mathbb{Z}), \mathbb{R})$$
 (D3)

where the last term $\text{Tor}(H_{r-1}(\mathbb{Z}), \mathbb{R})$ is the torsion product functor, which is defined as:

Definition 15 (Torsion product functor). Let \mathbb{Z} be the set of integers, and m be some integers. Then for a cyclic group \mathbb{Z}_m and another \mathbb{Z} -module R, $\text{Tor}(\mathbb{Z}_m, R) \cong [r \in R | mr = 0]$. In other words, it is the n-torsion subgroup of R.

We remark that this Tor is different from the Torsion that we used earlier. For convenience, we point out the following useful properties associated with Tor, and refer the readers to standard textbook for derivation.

Lemma 11 (Tor of \mathbb{Z} -modules). Let \mathbb{Z} be the set of integers, p be a prime number and R be some \mathbb{Z} -module.

- $\operatorname{Tor}(\mathbb{Z}, \mathbf{R}) = 0$
- Tor $(\bigoplus_{i} \mathbb{Z}_{m_i}, R) = \bigoplus_{i} \text{Tor } (\mathbb{Z}_{m_i}, R).$
- Let $\mathbb{F}_p \equiv \mathbb{Z}/p\mathbb{Z}$ be the finite field of size p. Then:

$$\operatorname{Tor}\left(\mathbb{Z}_{\mathrm{m}}, \mathbb{F}_{\mathrm{p}}\right) \cong \begin{cases} \mathbb{F}_{p} & \text{if } p \mid n \\ 0 & \text{if } p \nmid n \end{cases} \tag{D4}$$

• For arbitrary m (not necessarily a prime), it holds that:

$$\operatorname{Tor}(\mathbb{Z}_{n}, \mathbb{Z}_{m}) \cong \mathbb{Z}_{\gcd(m,n)}$$
 (D5)

• For $R = \mathbb{Q} - a$ divisible group, $\operatorname{Tor}(\mathbb{Z}_m, \mathbb{R}) = 0$ for any finite m.

Thus, a direct use of the above lemma leads us to:

$$H_r(\mathbb{R}) \cong H_r(\mathbb{Z}) \otimes_{\mathbb{Z}} \mathbb{R}$$
 (D6)

To proceed, we consider the term $H_r(\mathbb{Z}) \otimes_{\mathbb{Z}} \mathbb{R}$, which is:

$$H_r(\mathbb{Z}) \otimes_{\mathbb{Z}} \mathbb{R} \cong (\operatorname{Free}(H_r(\mathbb{Z})) \oplus \operatorname{Torsion}(H_r(\mathbb{Z}))) \otimes_{\mathbb{Z}} \mathbb{R}$$
 (D7)

$$= (\operatorname{Free}(H_r(\mathbb{Z})) \otimes_{\mathbb{Z}} \mathbb{R}) \oplus (\operatorname{Torsion}(H_r(\mathbb{Z})) \otimes_{\mathbb{Z}} \mathbb{R})$$
(D8)

We recall the properties from Lemma 10 that, for any integers m, $\mathbb{Z}_m \otimes_{\mathbb{Z}} Q = 0$ for any field Q of characteristic zero. At the same time, the torsion part $\text{Torsion}(H_r(\mathbb{Z}))$ is $\cong \mathbb{Z}_{d_1} \oplus \mathbb{Z}_{d_2} \oplus \cdots$, which results in

$$(Torsion(H_r(\mathbb{Z})) \otimes_{\mathbb{Z}} \mathbb{R}) = 0$$
 (D9)

For the first part $\operatorname{Free}(H_r(\mathbb{Z})) \otimes_{\mathbb{Z}} \mathbb{R}$, we can use the first property of Lemma 10, and also $\operatorname{Free}(H_r(\mathbb{Z})) \cong \mathbb{Z}^r$, which results in:

$$Free(H_r(\mathbb{Z})) \otimes_{\mathbb{Z}} \mathbb{R} \cong \mathbb{R}^r$$
 (D10)

which implies that

$$H_r(\mathbb{R}) \cong \mathbb{R}^r$$
 (D11)

suggesting that $H_r(\mathbb{R})$ behaves like a vector space. Thus, the above deduction reveals how the choice of coefficients influences the algebraic structure of homology, and that the typical choice of coefficients from \mathbb{R} or \mathbb{Z}_2 may hide the torsion part.

Appendix E: A few examples

To make the role of torsion clearer, we provide a few concrete examples showing how the torsion is intrinsic to topological space. We particularly provide specific topological spaces with their corresponding homology groups. We organize these examples into two categories; one contains torsion-free topological space, while the other contains spaces with torsion.

Torsion-free:

- Sphere S^n : $H_0(\mathbb{Z}) \cong \mathbb{Z}$, $H_n(\mathbb{Z}) \cong \mathbb{Z}$. For any $0 \leq m < n$, $H_m(\mathbb{Z}) \cong 0$.
- Torus T^n : $H_r(T^n, \mathbb{Z}) \cong \mathbb{Z}^{\binom{n}{k}}$.
- Closed orientable surfaces (with genus ≥ 1): $H_0(\mathbb{Z}) \cong \mathbb{Z}, H_1(\mathbb{Z}) \cong \mathbb{Z} \geq 2g, H_2(\mathbb{Z}) \cong \mathbb{Z}$.
- Complex projective space \mathbb{CP}^n : $H_{2k}(\mathbb{Z}) \cong \mathbb{Z}$ for $0 \leq k < n$; $H_{2k+1}(\mathbb{Z}) \cong 0$.
- Quaternionic projective space \mathbb{HP}^n : $H_{4k}(\mathbb{Z}) \cong \mathbb{Z}$ for $0 \leq k < n$. Otherwise 0.

Torsion:

- Real projective space \mathbb{RP}^n : $H_0(\mathbb{Z}) \cong \mathbb{Z}$. For $1 \leq i \leq n-1$, $H_i(\mathbb{Z}) \cong \mathbb{Z}_2$ if even i, and $H_i(\mathbb{Z}) \cong 0$ for odd i. $H_n(\mathbb{Z}) \cong \mathbb{Z}$ if n is odd, and $H_n(\mathbb{Z}) \cong 0$ if n is even.
- Lens space L(p,q) (3-manifolds): $H_0(\mathbb{Z}) \cong \mathbb{Z}$, $H_1(\mathbb{Z}) \cong \mathbb{Z}_p$, $H_2(\mathbb{Z}) \cong 0$, $H_3(\mathbb{Z}) \cong \mathbb{Z}$.
- Klein bottle $K: H_0(\mathbb{Z}) \cong \mathbb{Z}, H_1(\mathbb{Z}) \cong \mathbb{Z} \oplus \mathbb{Z}_2, H_2(\mathbb{Z})0.$
- Non-orientable close surface N_g (connected sum of g copies of \mathbb{RP}^2): $H_0(\mathbb{Z}) \cong 0, H_1(\mathbb{Z}) \cong \mathbb{Z}^{g-1} \oplus \mathbb{Z}_2, H_2(\mathbb{Z}) = 0.$
- Moorse space $M(\mathbb{Z}_m, n)$: $H_n(\mathbb{Z}) \cong \mathbb{Z}_m$.

Appendix F: Key insight

In the following, we describe the insight, which is a continuation of the previous section, that underlies our subsequently main algorithm to detect the possible torsion of a given simplicial complex, denoted K. Throughout the following, we omit this simplex notation K and naturally impose this setting. We recall from the previous section the universal coefficient theorem:

$$H_r(\mathbb{R}) \cong H_r(\mathbb{Z}) \otimes_{\mathbb{Z}} \mathbb{R} \oplus \text{Tor}(H_{r-1}(\mathbb{Z}), \mathbb{R})$$
 (F1)

which reflects the change in algebraic structure upon a change in the coefficients from \mathbb{Z} to \mathbb{R} . If instead of \mathbb{R} , we choose another ring/field Q, then the formula still holds:

$$H_r(Q) \cong H_r(\mathbb{Z}) \otimes_{\mathbb{Z}} Q \oplus \text{Tor}(H_{r-1}(\mathbb{Z}), Q)$$
 (F2)

According to Theorem 2, $H_r(\mathbb{Z})$ can be decomposed as:

$$H_r(\mathbb{Z}) \cong \mathbb{Z}^{\beta_r} \oplus \left(\bigoplus_i Z_{r_i}\right)$$
 (F3)

Then we have that the above formula is:

$$H_r(Q) \cong \left(\mathbb{Z}^{\beta_r} \otimes_{\mathbb{Z}} Q\right) \oplus \left(\bigoplus_i Z_{r_i} \otimes_{\mathbb{Z}} Q\right) \oplus \operatorname{Tor}\left(H_{r-1}(\mathbb{Z}), Q\right)$$
 (F4)

To make the above group become a vector space (since linear algebra is a more natural language in quantum computation), we choose Q to be some field. For a reason that will be clear later, we choose $Q = \mathbb{F}_p \equiv \mathbb{Z}/p\mathbb{Z}$ for p being a prime. Then for $Q = \mathbb{F}_p$, the above equation can be written as:

$$H_r(\mathbb{F}_p) \cong \left(\mathbb{Z}^{\beta_r} \otimes_{\mathbb{Z}} \mathbb{F}_p\right) \oplus \left(\bigoplus_i \mathbb{Z}_{r_i} \otimes_{\mathbb{Z}} \mathbb{F}_p\right) \oplus \operatorname{Tor}\left(H_{r-1}(\mathbb{Z}), \mathbb{F}_p\right)$$
 (F5)

Again, by Theorem 2, we have:

$$H_{r-1}(\mathbb{Z}) \cong \mathbb{Z}^{\beta_q} \oplus \left(\bigoplus_i Z_{q_i}\right)$$
 (F6)

Via Lemma 11, we have that:

$$\operatorname{Tor}\left(H_{r-1}(\mathbb{Z}), \mathbb{F}_{p}\right) \cong \operatorname{Tor}\left(\mathbb{Z}^{\beta_{q}} \oplus \left(\bigoplus_{i} Z_{q_{i}}\right), \mathbb{F}_{p}\right) \tag{F7}$$

$$\cong \operatorname{Tor}\left(\left(\bigoplus_{i} Z_{q_{i}}\right), \mathbb{F}_{p}\right)$$
 (F8)

$$\cong \bigoplus_{i,q_i|p} \mathbb{F}_p \tag{F9}$$

By Lemma 4, and also the fact that $\mathbb{F}_p \equiv \mathbb{Z}_p$, we have that:

$$\left(\bigoplus_{i} \mathbb{Z}_{k_i} \otimes_{\mathbb{Z}} \mathbb{F}_p\right) \cong \bigoplus_{i, k_i \mid p} \mathbb{F}_p \tag{F10}$$

$$\left(\mathbb{Z}^{\beta_r} \otimes_{\mathbb{Z}} \mathbb{F}_p\right) \cong \mathbb{F}_p^{\beta_r} \tag{F11}$$

Gathering everything, we have:

$$H_r(\mathbb{F}_p) \cong \mathbb{F}_p^{\beta_r} \oplus \left(\bigoplus_{i,r_i|p} \mathbb{F}_p\right) \oplus \left(\bigoplus_{i,q_i|p} \mathbb{F}_p\right)$$
 (F12)

We recall from the previous section that if we choose the field $Q \equiv \mathbb{R}$, then:

$$H_r(\mathbb{R}) \cong \mathbb{R}^{\beta_r}$$
 (F13)

It means that, the rank of the k-th homology space over \mathbb{F}_p field contains additional factors from the torsion part, i.e.,:

$$\dim\left(\mathbf{H}_{\mathbf{r}}(\mathbb{F}_{\mathbf{p}})\right) = \beta_{\mathbf{r}} + \mathbf{t}_{\mathbf{r}} + \mathbf{t}_{\mathbf{r}-1} \tag{F14}$$

where t_r, t_{r-1} is the sum of the cyclic summands (of k-th homology group/space and (k-1)-th homology group/space, respectively) of order divisible by a prime p. We recall from the previous section D that:

$$H_r(\mathbb{R}) \cong \mathbb{R}^{\beta_r}$$
 (F15)

which implies

$$\dim\left(H_r(\mathbb{R})\right) = \beta_r \tag{F16}$$

Our strategy is built on this, as we proceed to estimate the dimension of k-th homology group over two different fields \mathbb{R} and \mathbb{F}_p , and then compare them. If their dimensions are equal, then it indicates that there is no torsion. Otherwise, there is torsion. The problem then is, what value of p should we choose? We recall that p is a prime, and it is of a known fact that arbitrary integers can be decomposed as products of different primes. Thus, in general, without knowing the order of summands in advance (which is apparent, because if we know the order already, then the torsion is already known), the only strategy is to try as many primes as possible, e.g., p = 2, 3, 5..., 7, etc. In the following section, we construct a quantum algorithm to execute the estimation of the desired dimension, and subsequently, the comparison.

Appendix G: Quantum Algorithm

1. Input model

As seen from the main text, our input model being similar to the recent work [25], namely, the non-oracle model. Subsequently, we will also discuss how the oracle model can be used within our algorithm. Let $S_r = \{\sigma_{r_1}, \sigma_{r_2}, ...\}$

denotes the set of r-simplexes in the complex of interest K. For some r, let \mathcal{D}_r denotes the matrix of size $|\mathcal{S}_{r-1}| \times |\mathcal{S}_r|$, which encodes the structure of the given complex as follows. For a given column index, say j (with $1 \le j \le |\mathcal{S}_r|$), we have:

$$(\mathscr{D}_r)_{ij} = \begin{cases} 1 & \text{if } \sigma_{r_i} \cap \sigma_{(r-1)_j} \neq \emptyset \\ 0 & \text{if } \sigma_{r_i} \cap \sigma_{(r-1)_j} = \emptyset \end{cases}$$
 (G1)

Intuitively, the matrix \mathcal{D}_r encodes the local, mutual relations between all r-simplexes and (r-1)-simplexes. In addition, as a r-simplex shares r+1 faces with other (r-1)-simplexes, then for a given column, there are (r+1) nonzero entries. The assumption we make in our work is that the entries of $\{\mathcal{D}_r\}$ are classically known. We remark that the classically known entries is in the sense, or perspective of Lemma ??, where the entries can be efficiently loaded into a (large) quantum state.

As also discussed in [25], whether this model arises in practical scenario is unknown. However, in reality, we can achieve this model by directly specifying the simplexes. The method of specifying simplexes was also suggested in [23] as a mean to overcome a high-complexity subroutine required in the original LGZ algorithm. For instance, let K be the complex of interest and $v_0, v_1, ..., v_N$ be the N data points, or vertices in K. If we pick:

$$S_3 = [v_0, v_1, v_3], [v_2, v_3, v_7], [v_8, v_9, v_{16}], \tag{G2}$$

as 3-simplexes $\in K$, and:

$$S_2 = [v_0, v_1], [v_1, v_3], [v_0, v_3], [v_2, v_3], [v_3, v_7], [v_2, v_7], [v_8, v_9][v_8, v_{16}], [v_9, v_{16}], [v_5, v_7], [v_6, v_8]$$
(G3)

as 2-simplexes in $\in K$. Then we organize the above information as a matrix of size $|\mathcal{S}_2| \times |\mathcal{S}_3|$, resulting in the matrix \mathcal{D}_3 . The same construction holds for different orders, resulting in the matrices $\{\mathcal{D}_r\}$. In general, we can reformulate our problem as follows.

Given the classical knowledge of the matrix \mathscr{D}_r of size $|\mathcal{S}_{r-1}| \times |\mathcal{S}_r|$, with the property that any column has r+1 nonzero entries being 1. At the order r, does the simplicial complex K with structured encoded in this matrix have torsion?

2. Procedure

Earlier, we have mentioned the strategy for detecting torsion, which is based on comparing the dimension of r-th homology space/group H_k over two fields, \mathbb{R} and \mathbb{F}_p . Over \mathbb{R} , the dimension of $H_k(\mathbb{F}_p)$ is in fact the r-th Betti number commonly used in the literature. Yet, over \mathbb{F}_p , the dimension of $H_k(\mathbb{F}_p)$ can change, depending on whether the complex of interest has torsion. In the following, we discuss in detail the quantum algorithm for estimating the dimension of H_k over \mathbb{R} and \mathbb{F}_p . Before that, we provoke the following helpful lemma:

Lemma 12. Let U_A be a unitary block-encoding of a matrix $A \in \mathbb{C}^{N \times N}$ as in Definition 1. Let $|\phi_1\rangle = \frac{1}{||\phi_1||}\phi_1, |\phi_2\rangle = \frac{1}{||\phi_2||}\phi_2$ two quantum states of dimension N with a known preparation procedure. Then it holds that:

$$\langle \mathbf{0} | \langle \phi_2 | U_A | \mathbf{0} \rangle | \phi_1 \rangle = \langle \phi_2 | A | \phi_1 \rangle = \frac{1}{\|\phi_1\| \|\phi_2\|} \phi_2^{\dagger} A \phi_1$$
 (G4)

which can be estimated to some additive or multiplicative accuracy via Hadamard/SWAP test primitive.

To show this, we first observe that, according to Def 1, the action of U_A on $|\mathbf{0}\rangle |\phi_1\rangle$ is $U_A |\mathbf{0}\rangle |\phi_2\rangle = |\mathbf{0}\rangle A |\phi_2\rangle + |\text{Garbage}\rangle$ where $|\text{Garbage}\rangle$ is orthogonal to $|\mathbf{0}\rangle |\alpha\rangle$ for any α . Then by taking inner product:

$$\langle \mathbf{0} | \langle \phi_{2} | U_{A} | \mathbf{0} \rangle | \phi_{1} \rangle = \langle \mathbf{0} | \langle \phi_{2} | (|\mathbf{0}\rangle A | \phi_{1}\rangle + |\text{Garbage}\rangle)$$

$$= \langle \mathbf{0} | \langle \phi_{2} | | \mathbf{0} \rangle A | \phi_{1}\rangle + \langle \mathbf{0} | \langle \phi_{2} | |\text{Garbage}\rangle$$

$$= \langle \mathbf{0} | \langle \phi_{2} | | \mathbf{0} \rangle A | \phi_{1}\rangle$$
(G5)

By substituting $ket\phi_1 = \frac{1}{||\phi_1||} |\phi_1\rangle, |\phi_2\rangle = \frac{1}{||\phi_2||} |\phi_2\rangle$ to the above, we obtain the Lemma 12. The application of Hadamard/SWAP test primitive is straightforward, provided unitary U_A and state preparation routine for $|\phi_1\rangle, |\phi_2\rangle$.

Estimating β_r over real field \mathbb{R} . We first recall that the boundary operator is generally defined as:

$$\partial_r[p_0, p_1, \dots, p_r] = \sum_{i=0}^r (-1)^i [p_0, p_1, \dots, \hat{p_i}, \dots, p_r],$$
 (G6)

The classical knowledge of matrix \mathscr{D}_r translates to the classical knowledge of ∂_r directly, almost by definition. According to the above definition of boundary operator, ∂_r is of size $|\mathcal{S}_{r-1}| \times |\mathcal{S}_r|$. In the *j*-th column of ∂_r , which corresponds to the *j*-th *r*-simplex σ_{r_j} , the location of nonzero entries are those (r-1)-simplexes that are faces of σ_{r_j} . The value of these non-zero entries is either 1 or -1. Thus, from \mathscr{D}_r , we simply need to change the value of nonzero entries at certain locations from 1 to -1.

To proceed, we have seen earlier that the problem of estimating r-th Betti number, or normalized Betti number eventually reduce to estimating the kernel of the combinatorial Laplacian:

$$\Delta_r = \partial_{r+1} \partial_{r+1}^{\dagger} + \partial_r^{\dagger} \partial_r, \tag{G7}$$

This has already been applied in many previous works, e.g., [18–20, 23, 25, 26]. Thus, we refer the interested readers to each of them for concrete details. Here, we point out that all these works have different input assumptions and that our input model is similar to [25] (to some degrees, similar to [26] as well). Hence, it is most appropriate to use their result, as they also deal with a real field. We recapitulate the main procedure as well as the main result in [25] with regard to the estimation of the r-th Betti number over the real field \mathbb{R} in the following algorithm.

Algorithm 1 ([25]). Let $\{\mathscr{D}_r\}$ be the classical specification of the simplicial complex K of interest, having total N data points.

1. Use the classical knowledge of $\mathcal{D}_r, \mathcal{D}_{r+1}$ and Lemma 2 to construct the block-encoding of

$$\frac{1}{|\mathcal{S}_{r-1}||\mathcal{S}_r|} \partial_r^{\dagger} \partial_r, \frac{1}{|\mathcal{S}_r^K||\mathcal{S}_{r+1}|} \partial_{r+1} \partial_{r+1}^{\dagger}.$$

2. Then we use Lemma 6 to transform the block-encoded operators:

$$\frac{1}{|\mathcal{S}_{r-1}||\mathcal{S}_r|} \partial_r^{\dagger} \partial_r \longrightarrow \frac{1}{|\mathcal{S}_{r-1}||\mathcal{S}_r||\mathcal{S}_{r+1}|} \partial_r^{\dagger} \partial_r$$

$$\frac{1}{|\mathcal{S}_r||\mathcal{S}_{r+1}|} \partial_{r+1} \partial_{r+1}^{\dagger} \longrightarrow \frac{1}{|\mathcal{S}_{r-1}||\mathcal{S}_r||\mathcal{S}_{r+1}|} \partial_{r+1} \partial_{r+1}^{\dagger}$$

3. Use the block-encoding arithmetic recipes Lemma. 5 to construct the block-encoding of their summation, resulting in the block-encoding, denoted as U_r , of:

$$\frac{1}{2|\mathcal{S}_{r-1}||\mathcal{S}_r||\mathcal{S}_{r+1}|}\Delta_r \equiv \Delta_r'$$

where we define a new operator Δ'_r for simplicity. Of obvious fact, the rank of Δ'_r is equal to the rank of Δ_r .

- 4. Use stochastic rank estimation method proposed in [20, 34, 35] (see, e.g., Algo 3 in Appendix I) to estimate $\frac{\operatorname{rank}\Delta_{\mathbf{r}}}{|\mathcal{S}_{r}|}$. Specifically:
 - Draw s random states from Hadamard matrix (of corresponding dimension dim Δ_r) $|u_1\rangle$, $|u_2\rangle$, ..., $|u_s\rangle$ with i.i.d. entries and zero mean. According to [20], this can be done by randomly applying NOT gate on $\log \dim(\Delta_r)$ qubits, followed by an application of Hadamard gates to all qubits.
 - Use Lemma 9 with U_r (block-encoding of Δ'_r) to obtain the block-encoding of $T_j(\Delta'_r)$ for some $j \in \mathbb{Z}_+$ where $T_j(.)$ is the j-th Chebyshev polynomial.
 - For each i = 1, 2, ..., s, use Lemma 12 to estimate $\langle u_i, T_i(\Delta'_r)u_i \rangle$.
 - Compute:

$$\frac{1}{s} \sum_{i=1}^{s} \langle u_i | T_j(\Delta_r') | u_i \rangle \tag{G8}$$

$$\frac{1}{s} \sum_{j=0}^{m} \sum_{i=1}^{s} c_j \langle u_i | T_j(\Delta_r') | u_i \rangle$$
 (G9)

where $\{c_j\}_{j=1}^m$ being known factors.

Output: the estimator $\hat{r} = \sum_{j=0}^{m} \sum_{i=1}^{s} c_j \langle u_i | T_j(\Delta'_r) | u_i \rangle$.

Guarantee: Assuming that the eigenvalues of Δ'_r are $\in (\frac{1}{\kappa_{\Delta'_r}}, 1)$. For $s = \mathcal{O}\left(\frac{1}{\epsilon^2}\log\frac{1}{\delta}\right)$, and $m = \mathcal{O}\left(\log\frac{\kappa_{\Delta'_r}}{\epsilon}\right)$, then according to [34, 35], with a failure probability δ , it holds that $|\hat{r} - \frac{\operatorname{rank}(\Delta'_r)}{\dim(\Delta'_r)}| \leq \epsilon$. As the rank of Δ'_r is the same as the rank of Δ_r , and $\dim(\Delta'_r) = \dim(\Delta_r) = |\mathcal{S}_r|$ then \hat{r} also satisfies:

$$\left| \hat{r} - \frac{\operatorname{rank}(\Delta_{\mathrm{r}})}{|\mathcal{S}_r|} \right| \le \epsilon \tag{G10}$$

A more completed analysis of the algorithm above can be found in [25]. We recapitulate the main result in the following:

Lemma 13 ([25]). Assuming the eigenvalues of the combinatorial Δ_r having magnitude $\in (\frac{1}{\kappa \Delta_r}, 1)$, which implies that the eigenvalues of

$$\Delta_r' \equiv \frac{1}{2|\mathcal{S}_{r-1}||\mathcal{S}_r||\mathcal{S}_{r+1}|} \Delta_r$$

having magnitudes within

$$\left(\frac{1}{2|\mathcal{S}_{r-1}||\mathcal{S}_r||\mathcal{S}_{r+1}|\kappa_{\Delta_r}},1\right)$$

Then the Algorithm 1 outputs an estimation of the r-th normalized Betti number $\frac{\beta_r}{|S_r|}$ to additive precision ϵ , with success probability $1 - \delta$, with time complexity

$$\mathcal{O}\left(\log(|\mathcal{S}_{r-1}||\mathcal{S}_r|)\log\left(\kappa_{\Delta_r}|\mathcal{S}_{r-1}||\mathcal{S}_r||\mathcal{S}_{r+1}|\right)\frac{1}{\epsilon^2}\log\left(\frac{1}{\delta}\right)\right) \\
\in \mathcal{O}\left(\log(|\mathcal{S}_{r-1}||\mathcal{S}_r|)\log\left(\kappa_{\Delta_r}r|\mathcal{S}_{r-1}||\mathcal{S}_r||\mathcal{S}_{r+1}|\right)\frac{1}{\epsilon^2}\log\left(\frac{1}{\delta}\right)\right) \tag{G11}$$

In addition, we point out that in the same work [25], the authors also proposed an alternative way to estimate Betti numbers, based on the tracking of different homology classes.

Estimating β_r over \mathbb{F}_p . We remind the readers that the boundary operator is:

$$\partial_r[p_0, p_1, \dots, p_r] = \sum_{i=0}^r (-1)^i [p_0, p_1, \dots, \hat{p_i}, \dots, p_r],$$
 (G12)

Over real field \mathbb{R} , complex field \mathbb{C} , or integer ring \mathbb{Z} , -1 is the inverse element of 1 in the usual sense that we use. Over finite field, however, things are different. The inverse element, say of 1, is no longer -1, because in this case, for example, $\mathbb{F}_p \equiv \mathbb{Z}/p\mathbb{Z}$, that -1 does not even belong to this set. Instead, we need to rely on the definition provided in the Appendix B. It states that the inverse of an element, say x, of an Abelian group \mathcal{G} (with group operation +) is another element y such that x + y = 0 where 0 is the identity element. We consider the case $\mathbb{Z}/2\mathbb{Z}$, which contains of two element $\{0,1\}$. Then it can be seen that 1+1=0 (module 2), thus suggesting that in this group $\mathbb{Z}/2\mathbb{Z}$, 1 is its own inverse element. More generally, let $\mathbb{F}_p \equiv (0,1,2,...,p-1)$ (with the group operation taken modulo p), then the inverse element of 1 in \mathbb{F}_p is p-1. Thus, over a finite field \mathbb{F}_p , the entries with value 1 remains the same, and value -1 in the boundary map ∂_r is replaced by p-1, and all the subsequent arithmetic operation needs to be done modulo p. However, we point out that equivalently, we can define:

$$\mathbb{F}_p \equiv \left(\frac{-(p-1)}{2}, \cdots, -1, 0, 1, \cdots \frac{p-1}{2}\right) \tag{G13}$$

In this setup, the value of 1, -1 remain the same, only that the arithmetic operation needs to be done modulo p. Therefore, it is not hard to see that the matrix representation of boundary operator remains in this finite field case.

The next goal is to estimate the dimension of r-th homology group H_r over \mathbb{F}_p , which is also the main challenge when we change from real field \mathbb{R} to \mathbb{F}_p . To be more specific, at the third step of Algorithm 1, there is an application of stochastic rank estimation method originally derived from [34, 35], and this method only works on real, or complex

field \mathbb{C} . Likewise, other quantum algorithms for estimating Betti numbers, such as [18, 19, 23], are based on quantum simulation and quantum phase estimation, which are built naturally on complex field \mathbb{C} .

To this end, we point out that there is a relevant attempt in developing classically randomized algorithms to estimate the rank of a matrix [47, 48] over finite field. The idea and mechanism of these algorithms are very similar to the stochastic rank estimation method proposed in [34, 35], as they also generate a sequence of vectors with random entries. The rank of the matrix of interest, say A, is deducted from the action of A on these randomized vectors. The only difference is that, eventually, the arithmetic operations need to be done modulo p. We leave the details of these algorithms in the Appendix I, where we will provide a concrete procedure of two algorithms to estimate rank, in the infinite case (like \mathbb{R}_p ; see Algorithm 3) and the finite case (like \mathbb{F}_p ; see Algorithm 4). In the following, we formally describe our quantum algorithm for estimating the rank of a block-encoded matrix in a finite field, based on the classical algorithm Algo 4.

Algorithm 2 (Quantum algorithm for estimating rank in finite field). Let $\{\mathscr{D}_r\}$ be the classical specification of the simplicial complex K of interest, and \mathbb{F}_p be the finite field of interest.

1. Use the classical knowledge of $\mathcal{D}_r, \mathcal{D}_{r+1}$ and Lemma 2 to construct the block-encoding of

$$\frac{1}{|\mathcal{S}_{r-1}||\mathcal{S}_r|}\partial_r^{\dagger}\partial_r, \frac{1}{|\mathcal{S}_r||\mathcal{S}_{r+1}|}\partial_{r+1}\partial_{r+1}^{\dagger}.$$

Denote the above unitaries as U_r, U_{r+1} respectively.

- 2. Use Lemma 1 to generate t different quantum states $|v_1\rangle, |v_2\rangle, ..., |v_t\rangle$ with randomly i.i.d. entries drawn from \mathbb{F}_p . Likewise, generating s different quantum states $|u_1\rangle, |u_2\rangle, ..., |u_s\rangle$ with randomly i.i.d. entries drawn from \mathbb{F}_p .
- 3. For all i = 1, 2, ..., t, and j = 1, 2, ..., s, use Lemma 12 to estimate the overlaps:

$$\langle \mathbf{0} | \langle u_i | U_r | \mathbf{0} \rangle | v_j \rangle = \frac{1}{||u_i|| \ ||v_j||} u_i^{\dagger} \partial_r^{\dagger} \partial_r v_j$$

$$= \frac{1}{2||u_i|| \ ||v_j|||\mathcal{S}_r||\mathcal{S}_{r-1}|} u_i^{\dagger} \Delta_r v_j$$
(G14)

with a chosen additive precision

$$\epsilon = \frac{1}{4||u_i|| \ ||v_i|||\mathcal{S}_r||\mathcal{S}_{r-1}|}.$$

Similarly, estimate the overlaps $\langle \mathbf{0} | \langle u_i | U_{r+1} | \mathbf{0} \rangle | v_i \rangle$ to the same precision ϵ .

4. For all i = 1, 2, ..., t, and j = 1, 2, ..., s, infer the value:

$$u_i^{\dagger} \partial_r^{\dagger} \partial_r v_j = ||u_i|| \cdot ||v_j|| 2|\mathcal{S}_r| (|\mathcal{S}_{r-1}| + |\mathcal{S}_{r+1}|) \langle \mathbf{0}| \langle u_i| U_r |v_j \rangle$$
(G15)

By choosing

$$\epsilon = \frac{\eta |u_i^{\dagger} \partial_r^{\dagger} \partial_r v_j|}{4||u_i|| \ ||v_j|||\mathcal{S}_r||\mathcal{S}_{r-1}|}$$

the estimation of $u_i^{\dagger} \partial_r^{\dagger} \partial_r v_j$ has an multiplicative accuracy η . Similarly, the estimation of $u_i^{\dagger} \partial_{r+1} \partial_{r+1}^{\dagger} v_j$ can be estimated to the same accuracy. Then we add them to form the estimation of $u_i^{\dagger} \partial_r^{\dagger} \partial_r v_j + u_i^{\dagger} \partial_{r+1} \partial_{r+1}^{\dagger} v_j = u_i^{\dagger} \Delta_r v_j$ to the same multiplicative accuracy η .

- 5. Taking the estimated value above modulo p. Then we obtain $u_i^{\dagger} \Delta_r v_i \pmod{p}$.
- 6. Classically build the matrix M with $M_{ij} = u_i^{\dagger} \Delta_r v_j \pmod{p}$. Then find its rank rank(M) via classical Gaussian elimination modulo p.

Output: $\hat{r} = \text{rank}(M)$.

Guarantee: For $s, t = \mathcal{O}\left(\log_p \frac{1}{\delta}\right)$ and the entries of V, U are random with i.i.d. uniform over \mathbb{F}_p , the above estimation of \hat{r} succeeds with probability:

$$Prob[\hat{\mathbf{r}} = \mathbf{r}] > 1 - \delta \tag{G16}$$

The quantum algorithm for torsion detection is a direct application of Algorithm 1 and 2.

- Repeat the Algorithm 2 for various values of prime p, we obtain a sequence of estimators $\hat{r}_{p_1}, \hat{r}_{p_2},, \hat{r}_{p_K}$
- Compare the values $\hat{r}_{p_1}, \hat{r}_{p_2},, \hat{r}_{p_K}$ and also the value of $\frac{\mathrm{rank}\Delta_r}{|\mathcal{S}_r|}$ estimated via Algorithm 1.

Output: If there are differences \longrightarrow complex K has torsion (at order r). Otherwise, it does not have torsion.

3. Extension to oracle-based input model

We recall that the input information to our algorithm is the classical knowledge of matrices $\{\mathcal{D}_r\}$ encoding the mutual relation between r-simplexes and (r-1)-simplexes. This classical knowledge allows us to leverage the result of [45] (see Lemma 2) to block-encode the operator that is $\propto \Delta_r$, as well as subsequently, $\Delta_r^{\text{mod p}}$. As mentioned earlier, existing works on quantum TDA have different input assumptions. Many, if not most of them, such as [18–20, 22], encode the simplexes of the given complex into the computational basis states of appropriate qubits system. For instance, assuming that the complex K has N data points. Let $v_1, v_2, ..., v_N$ denotes these N data points, or 0-simplexes. Then a 1-simplex $[v_i, v_j]$ is encoded to the computational basis state of N-qubits system, that has the bit at position i and j equal to 1, and 0 otherwise. Likewise, a 2-simplex $[v_i, v_j, v_k]$ is encoded to the basis state that has the bit 1 at position i, j, k, and 0 otherwise. Generally, a r-simplexes is encoded into a string of Hamming weight r+1. In addition, another enabling component of these algorithms is the oracle O_r , which acts on a string σ_r of Hamming weight r+1 as follows:

$$O_r |0\rangle |\sigma_r\rangle = \begin{cases} |1\rangle |\sigma_r\rangle & \text{if } \sigma_r \in \mathcal{K} \\ |0\rangle |\sigma_r\rangle & \text{otherwise} \end{cases}$$
 (G17)

One can see that the above oracle is similar to the oracle in the Grover algorithm. In fact, the algorithm in [18–20, 22] employs a multi-solution version of Grover's search algorithm as a subroutine.

The integration of the above oracle with our algorithm is quite straightforward as a corollary of a technique introduced [22]. Specifically, in Section 6, they show the following:

Lemma 14 (Section 6 of [22]). Provided the oracle O_r as above, then there is a quantum circuit of complexity $\mathcal{O}(N^2)$ that is an exact block-encoding of $\frac{\partial_r}{N(r+1)}$.

Thus, we can use the above result to obtain the block-encoding of:

$$\frac{\partial_r}{N(r+1)}, \frac{\partial_r^{\dagger}}{N(r+1)}, \frac{\partial_{r+1}}{N(r+2)}, \frac{\partial_{r+1}^{\dagger}}{N(r+2)}$$
(G18)

Then we use Lemma 3 to construct the block-encoding of

$$\frac{1}{N^2(r+1)^2}\partial_r^\dagger\partial_r, \frac{1}{N^2(r+2)^2}\partial_{r+1}\partial_{r+1}^\dagger$$

From here, can execute a similar procedure as Algo. 2 to find out the rank of Δ_r over various p, then compare them in order to detect torsion.

Appendix H: Complexity and Error Analysis

In this section, we provide a detailed discussion on the overall error and complexity of the algorithm outlined above (the non-oracle case). We will follow exactly each step of the algorithm 2 and explicitly detail the complexity of the recipes used in each step. An analysis for the oracle case will be given afterward.

1. Analysis for non-oracle case

Step 1: We first point out that the operator \mathscr{D}_r has size $|\mathcal{S}_{r-1}| \times |\mathcal{S}_r|$. Thus, an application of Lemma 2 uses a quantum circuit of depth, respectively

$$\mathcal{O}\left(\log|\mathcal{S}_{r-1}||\mathcal{S}_r|\right), \mathcal{O}\left(\log|\mathcal{S}_{r+1}||\mathcal{S}_r|\right) \tag{H1}$$

Step 2: At this step, we use Lemma 1 to prepare the states (of dimension $|S_r|$) with randomly i.i.d. entries drawn from \mathbb{F}_p , which use a quantum circuit of depth:

$$\mathcal{O}\left(\log|\mathcal{S}_r|\right) \tag{H2}$$

Step 3 & 4 & 5: In the first two steps, we need to use the block-encoding from the previous two steps, inside the Hadamard/SWAP test primitive, to estimate the overlaps:

$$\langle \mathbf{0} | \langle u_i | U_r | \mathbf{0} \rangle | v_j \rangle = \frac{1}{||u_i|| \ ||v_j|| |\mathcal{S}_r|(|\mathcal{S}_{r-1}| + |\mathcal{S}_{r+1}|)} u_i^{\dagger} \partial_r^{\dagger} \partial_r v_j \tag{H3}$$

with an additive precision

$$\epsilon = \frac{\eta |u_i^{\dagger} \partial_r^{\dagger} \partial_r v_j|}{4||u_i|| \ ||v_j|||\mathcal{S}_r||\mathcal{S}_{r-1}|}$$

which implies an estimation of $u_i^{\dagger} \partial_r^{\dagger} \partial_r v_j$ with multiplicative accuracy η . Because $u_i^{\dagger} \partial_r^{\dagger} \partial_r v_j$ is an integer, it can be inferred from the estimation above by choosing $\eta = \frac{1}{2}$. For example, with such a multiplicative precision, we simply need to round the estimation above to the nearest integer. We note that the primitives above use amplitude estimation as a subroutine. As such, we can use the recent results [49–51] which bypass the need of the quantum Fourier transform compared to the traditional methods. Provided that the circuit depth of the block-encoding of

$$\frac{\partial_r^{\dagger} \partial_r}{|\mathcal{S}_r||\mathcal{S}_{r-1}|}$$

and of $|u_i\rangle$, $|v_i\rangle$ are, respectively:

$$\mathcal{O}\left(\log|\mathcal{S}_{r-1}||\mathcal{S}_r|\right), \ \mathcal{O}\left(\log|\mathcal{S}_r|\right)$$
 (H4)

The estimation above has circuit complexity

$$\mathcal{O}\left(\log|\mathcal{S}_{r-1}||\mathcal{S}_r|\frac{1}{\eta}\sqrt{\frac{2||u_i||\ ||v_j|||\mathcal{S}_r||\mathcal{S}_{r-1}|}{u_i^{\dagger}\partial_r^{\dagger}\partial_r v_j}}\right).$$

We remark on the following property:

$$\frac{u_i^{\dagger} \partial_r^{\dagger} \partial_r v_j}{||u_i|| \ ||v_j||} = \langle u_i | \partial_r^{\dagger} \partial_r | v_j \rangle \tag{H5}$$

Under the promise that ∂_r (and hence, $\partial_r^{\dagger}\partial_r$) has eigenvalues bounded, the above quantity can be safely treated as $\mathcal{O}(1)$. Therefore, the circuit complexity above is simplified further as:

$$\mathcal{O}\left(\log\left(|\mathcal{S}_{r-1}||\mathcal{S}_r|\right)\frac{1}{\eta}\sqrt{|\mathcal{S}_r|\left(|\mathcal{S}_{r-1}|\right)}\right).$$

Similarly, the estimation of $u_i^{\dagger} \partial_{r+1} \partial_{r+1}^{\dagger} v_j$ to the same multiplicative accuracy η has complexity

$$\mathcal{O}\left(\log\left(|\mathcal{S}_{r+1}||\mathcal{S}_r|\right)\frac{1}{\eta}\sqrt{|\mathcal{S}_r||\mathcal{S}_{r+1}|}\right).$$

For simplicity, we define $S_r^{\max} = \max\{|\mathcal{S}_{r+1}|, |\mathcal{S}_r|, \mathcal{S}_{r-1}|\}$. The total complexity in the above estimations is:

$$\mathcal{O}\left(\log\left(S_r^{\max}\right)\frac{1}{\eta}S_r^{\max}\right)$$

As the last **Step 5**, taking modulo p of $u_i^{\dagger} \Delta_r v_j$. As we need to evaluate $u_i^{\dagger} \Delta_r v_j$ (mod p) for i=1,2,...,t, j=1,2,...,s, so we need to repeat the above process $s \cdot t = \mathcal{O}\left((\log_p \frac{1}{\delta})^2\right)$ times. **Step 6& 7 & 8:** Performing Gaussian elimination on a matrix of size $m \times n$ has complexity $\mathcal{O}(mn)$ [58]. So the

complexity for finding the rank of $M \pmod{p}$ is $\mathcal{O}(st) \in \mathcal{O}\left((\log_n \frac{1}{\delta})^2\right)$.

Summary. To sum up, for a fixed multiplicative accuracy η , our algorithm makes use of a quantum circuit of maximum complexity

$$\mathcal{O}\left(\log\left(S_r^{\max}\right)\frac{1}{\eta}S_r^{\max}\right) \tag{H6}$$

and need to repeat such circuit $\mathcal{O}\left(\log_p^2 \frac{1}{\delta}\right)$ times, assisted by a classical routine of complexity

$$\mathcal{O}\left(\log_p^2 \frac{1}{\delta}\right)$$
.

2. Analysis for oracle case

While the above complexity analysis is for the non-oracle case, the complexity analysis for the oracle case can be carried out in a straightforward manner. The only difference is that, in the **Step 1**, we use the result of [22] to obtain the block-encoding of $\frac{\partial_r}{N(r+1)}$. The complexity of these two steps is $\mathcal{O}(N^2)$. From the **Step 2** onward, the procedure is the same, with merely the interchange between $|\mathcal{S}_r||\mathcal{S}_{r-1}| \leftrightarrow N^2(r+1)^2$ and $|\mathcal{S}_r||\mathcal{S}_{r+1}| \leftrightarrow N^2(r+2)^2$. Thus the complexity can be deduced in a straightforward manner. To sum up, we have that the quantum circuit complexity in the oracle case is:

$$\mathcal{O}\left(\left(N^2 + \log|\mathcal{S}_r|\right) \frac{1}{\eta} Nr\right) \tag{H7}$$

The total of iterations is $st = \mathcal{O}\left(\left(\log_p \frac{1}{\delta}\right)^2\right)$ for a success probability $1 - \delta$, followed by a classical algorithm of complexity

$$\mathcal{O}\left(\log_p^2 \frac{1}{\delta}\right)$$
.

Appendix I: Classical Randomized Algorithm for Rank Estimation

For convenience, we provide a neat summary, or pipeline of the two algorithms for rank estimation over infinite and finite field, respectively. We refer the interested readers to the correspondingly original works for a more rigorous treatment.

The first one is the stochastic rank estimation proposed in [20, 34, 35]. The method is based on the property that rank $A \equiv \text{Tr}(h(A))$ where h(x) is a step function for $x \in (-1,1)$. The step function is then approximated by Chebyshev polynomial $h(x) \approx \sum_{j=0}^{m} c_j T_j(x)$ where $T_j(.)$ is the Chebyshev polynomial.

Algorithm 3 (Rank estimation over \mathbb{R}/\mathbb{C} [34, 35]). Let $A \in \mathbb{R}^{n \times n}/\mathbb{C}^{n \times n}$ be a Hermitian matrix with eigenvalues having magnitude $\in (\frac{1}{\kappa_n}, 1)$.

- 1. Draw s random vectors $u_1, u_2, ..., u_s \in \mathbb{R}^n$ with i.i.d. entries $\in \mathbb{R}/\mathbb{C}$.
- 2. For each i = 1, 2, ..., s, compute $\langle u_i, T_i(A)u_i \rangle$ where $T_i(.)$ is the Chebyshev polynomial.
- 3. Compute:

$$\frac{1}{s} \sum_{i=1}^{s} u_i^{\dagger} T_j(A) u_i \tag{I1}$$

$$\frac{1}{s} \sum_{j=0}^{m} \sum_{i=1}^{s} c_j u_i^{\dagger} T_j(A) u_i \tag{I2}$$

Output: $\hat{r} = \sum_{i=0}^{m} \sum_{i=1}^{s} c_j u_i^{\dagger} T_j(A) u_i$ is the estimator for the rank of A.

Guarantee: For $s = \mathcal{O}\left(\frac{1}{\epsilon^2}\log\frac{1}{\delta}\right)$, $m = \mathcal{O}\left(\log\frac{\kappa_A}{\epsilon}\right)$, with a success probability $\geq 1 - \delta$, it holds that:

$$|\hat{r} - r| \le \epsilon \tag{I3}$$

Time complexity: $\mathcal{O}\left(n^2 \frac{1}{\epsilon^2} \log\left(\frac{1}{\delta}\right) \log \frac{\kappa_A}{\epsilon}\right)$

As can be seen, the above method is based on the approximation of rank(A) as a trace of certain function of A (the step function). The trace is then approximated by a polynomial of corresponding matrix. An important ingredient in the above algorithm is the first step. As pointed out in [34, 35], any random vector with zero mean and i.i.d. coordinates can work. To obtain such a sequence of random vectors, the authors in [20] proposed to randomly draw columns from the Hadamard matrix. As emphasized in [20], this choice works very well in practical setting. To achieve this, they began with the state $|0\rangle^{\log n}$, followed by a random application of NOT gate in each of the $\log n$ qubits, and then Hadamard gates to all $\log n$ qubits. Repeating this process s times results in random Hadamard states $|u_1\rangle, |u_2\rangle, ..., |u_s\rangle$, which is sufficient for the purpose of trace and rank estimation in the above algorithm. To be more precise, since the states $|u_1\rangle, |u_2\rangle, ..., |u_s\rangle$ are normalized, the estimation $\frac{1}{s}\sum_{j=0}^{m}\sum_{i=1}^{s}c_j\langle u_i|T_j(A)|u_i\rangle$ actually approximate $\frac{\text{Tr}A}{N}$.

It can be seen that the above discussion does not hold in the finite case, as we cannot approximate the trace and rank via Chebyshev polynomials. To this end, it turns out that there are multiple classical algorithms tailored for finite case. In the following, we provide a summary/pipeline of the method introduced in [47, 48].

Algorithm 4 (Rank Estimation Over \mathbb{F}_p [47, 48]). Let $A \in \mathbb{F}_p^{n \times n}$ be a matrix of size $m \times n$ over the field \mathbb{F}_p . Let r denotes the rank of A.

- 1. Draw t random vectors $v_1, v_2, ..., v_t \in \mathbb{F}_n^n$. Define V be a matrix of size $n \times t$, with $[v_1, v_2, ..., v_t]$ as columns.
- 2. Draw s random vectors $u_1, u_2, ..., u_s \in \mathbb{F}_p^n$. Define U be a matrix of size $s \times n$, with $[u_1^T, u_2^T, ..., u_s^T]$ as rows.
- 3. Define a matrix M of size $s \times t$ with entries:

$$M_{ij} = u_i^T A v_j \pmod{p} \tag{I4}$$

Or equivalently

$$M = UAV (I5)$$

4. Find rank \hat{r} of M (via Gaussian elimination mod p).

Output: \hat{r} is an estimator for the rank of M.

Guarantee: For $s,t=\mathcal{O}\left(\log_p\frac{1}{\delta}\right)$ and the entries of V,U are random with i.i.d. uniform over \mathbb{F}_p , the above estimation of \hat{r} succeeds with probability:

$$Prob[\hat{\mathbf{r}} = \mathbf{r}] \ge 1 - \delta \tag{I6}$$

Time complexity: $\mathcal{O}\left(n^2 \log \frac{1}{\delta}\right)$

Appendix J: Proof of Lemma 2 and Lemma 1

We remark that Lemma 2 is the result of [25], which is based on [45]. The original proof can thus be found in Appendix C of [25]. Here, for completeness, we directly quote their proof to aid the interested readers.

1. General framework [45]

As mentioned, Lemma 2 can be seen as a corollary of a recent result [45], which generally shows that it is possible to block-encode a matrix (up to a scaling factor) provided its classical description, or its entries. First, we point out the following property. Let A be a matrix of size $M \times N$. Let A^i denotes the i-th column of A. Then consider the following vector (not necessarily normalized)

$$\frac{1}{\sqrt{MN}} \sum_{i=1}^{N} \underbrace{A^{i}}_{\text{register1}} |i\rangle \tag{J1}$$

is of dimension MN. If we trace out the first register in the above vector, we obtain the following operator:

$$\frac{1}{MN}A^{\dagger}A\tag{J2}$$

Our goal is to construct the block-encoding of the above operator, provided the classical knowledge, or the entries of A. Before describing the procedure, we mention a helpful lemma:

Lemma 15 ([46] Block Encoding Density Matrix). Let $\rho = \operatorname{Tr}_A |\Phi\rangle \langle \Phi|$, where $\rho \in \mathbb{H}_B$, $|\Phi\rangle \in \mathbb{H}_A \otimes \mathbb{H}_B$. Given unitary U that generates $|\Phi\rangle$ from $|\mathbf{0}\rangle_A \otimes |\mathbf{0}\rangle_B$, then there exists a highly efficient procedure that constructs an exact unitary block encoding of ρ using U and U^{\dagger} a single time, respectively.

Approach 1 – based on [39]. The state preparation method in [39] achieves efficient depth while using a modest number of ancilla at the same time. Specifically, according to the description below the Theorem 1 in [39], let $f: [-a, a] \longrightarrow \mathbb{R}$ be a (preferably smooth) function of arbitrary parity, and define:

$$|\Phi_f\rangle = \frac{1}{\mathcal{N}_f} \sum_{i=-\frac{N}{2}}^{\frac{N}{2}-1} f\left(\frac{2ai}{N}\right)|i\rangle$$

where $\mathcal{N}_f = \sqrt{\sum_i f(.)^2}$. Then there exists a deterministic procedure (see Figure 1 of [39]) that prepares the state:

$$\frac{1}{\sqrt{N}}|00\rangle \sum_{i}^{N} f\left(\frac{2ai}{N}\right)|i\rangle + |\text{Garbage}\rangle \tag{J3}$$

where $|\text{Garbage}\rangle$ refers to the redundant part that is completely orthogonal to the first part $|00\rangle\sum_i^N f\left(\frac{2ai}{N}\right)|i\rangle$. The quantum circuit complexity of the above procedure is $\mathcal{O}(\deg(f)\log N)$ (where $\deg(f)$ is the degree of function f), with extra 3 ancilla qubits. We remark that in the above, it was mentioned that the function f being smooth. As discussed in [39], their method can also be simply extended to non-smooth functions as well, with asymptotically the same complexity. To obtain the state $|\Phi_f\rangle$, we measure the ancilla and post-select $|00\rangle$. The success probability of this measurement is $\mathcal{O}\left(\frac{N_f}{N}\right)$. By using oblivious amplitude amplification, which incurs the quantum circuit complexity by a factor $\sim \sqrt{\frac{N}{N_f}}$, the success probability of the measurement is close to unity. Therefore, the total circuit complexity for obtaining $|\Phi_f\rangle$ is $\mathcal{O}\left(\sqrt{\frac{N}{N_f}}\deg(f)\log N\right)$.

To apply the above result, we first promote the new variable k = j + (i - 1)N, which has the property: $|k\rangle = |j + (i - 1)N\rangle = |j\rangle |i\rangle$. Then there is a correspondence between states $\sum_{i,j=1}^{N,M} A_{ij} |j\rangle |i\rangle = \sum_{k=1}^{N^2} a_k |k\rangle$ where the new amplitude $a_k \equiv a_{j+(i-1)N} = A_{ji}$. For any (preferably smooth) function $f: [-1,1] \longrightarrow [-1,1]$, if the entries $\{a_k\}_{k=1}^{MN}$ obey $a_k = f(\frac{k}{MN}) = f(j+(i-1)N) = A_{ji}$, then as mentioned earlier, there exists a deterministic procedure that prepares the state:

$$\frac{1}{\sqrt{MN}} |00\rangle \sum_{k=1}^{MN} f(\frac{k}{MN}) |k\rangle + |\text{Garbage}\rangle$$

$$= \frac{1}{\sqrt{MN}} |00\rangle \sum_{k=1}^{MN} a_k |k\rangle + |\text{Garbage}\rangle$$

$$= \frac{1}{\sqrt{MN}} |00\rangle \sum_{i,j=1}^{N,M} A_{ji} |j\rangle |i\rangle + |\text{Garbage}\rangle$$

$$= \frac{1}{\sqrt{MN}} |00\rangle \sum_{i,j=1}^{N} A^i |i\rangle + |\text{Garbage}\rangle$$

$$= \frac{1}{\sqrt{MN}} |00\rangle \sum_{i}^{N} A^i |i\rangle + |\text{Garbage}\rangle$$

The above state can be achieved using a quantum circuit having gate complexity $\mathcal{O}(\deg(f)\log MN)$ (where $\deg(f)$ is the degree of function f) and 3 ancilla qubits. We comment that in the above, we have assumed that there is a function f satisfying the stated condition. In principle, there can be many possible choices of f. Subsequently, in Appendix J3 (see the paragraph above Appendix K), we will discuss an effective route to obtain the function f as desired, provided the classical knowledge of $\{A_{ij}\}$.

To obtain the block-ending of $\sim A^{\dagger}A$ from the above state, we append another ancilla initialized in $|00\rangle$ to the state above, so we have the state:

$$\frac{1}{\sqrt{MN}} \sum_{i}^{N} \underbrace{|00\rangle}_{\text{register 1 register 2}} \underbrace{|00\rangle}_{\text{register 2}} A^{i} |i\rangle + |00\rangle |\text{Garbage}\rangle \tag{J5}$$

followed by two CNOT gates between register 1 and 2. Then we obtain the state:

$$\frac{1}{\sqrt{MN}} |00\rangle \sum_{i}^{N} \underbrace{|00\rangle A^{i}}_{\text{registerX}} |i\rangle + |\text{Garbage'}\rangle |\text{Garbage}\rangle$$
 (J6)

where $|\text{Garbage'}\rangle$ is completely orthogonal to $|00\rangle$. As we pointed out earlier, if we trace out the first register of the vector $\frac{1}{\sqrt{MN}}\sum_{i}^{N}A^{i}|i\rangle$, then we obtain the operator $\frac{1}{MN}A^{\dagger}A$. As such, if we trace out the register X in the state above, we obtain the density state:

$$|00\rangle\langle 00| \otimes \frac{1}{MN} A^{\dagger} A + (...)$$
 (J7)

where (...) refers to the redundant part. The density state above can be block-encoded via the Lemma 15. According to Definition 1, this density state is also the block-encoding of $\frac{1}{MN}A^{\dagger}A$, thus implying that we have achieved the desired block-encoding.

Recall that the quantum circuit complexity of preparing the state in Eqn. J4 is $\mathcal{O}(\log MN)$ (we assume $\deg(f) = \mathcal{O}(1)$). The adding of two more ancilla qubits $|00\rangle$ and usage of 2 CNOT gates increases the circuit complexity by $\mathcal{O}(1)$. Finally, the application of Lemma 15 uses the state preparation unitary in Eqn. J4 one more, thus the total circuit complexity is $\mathcal{O}(\log MN)$.

Approach 2 – based on [38, 59]. In the above procedure, we used the state preparation method in [39] to prepare the state that contains $\sim \sum_{i,j=1}^{N,M} A_{ji} |j\rangle |i\rangle$ as a subvector. However, we remark that other state preparation methods exist. For example, the method in [38, 59] considers the state of the form $\sum_{i=1}^{N} f(i) |i\rangle$ where $f:[0,1]:\longrightarrow \mathbb{R}_+$ is a continuous, positively integrable function satisfying $\sum_{i=1}^{N} f(i)^2 = 1$. They show that if f(.) is efficiently integrable, then $\sum_{i=1}^{N} f(i) |i\rangle$ can be prepared, with a fidelity ϵ , using a log N-qubit quantum circuit of complexity $\mathcal{O}\left(2^{k(\epsilon)}\right)$, where

$$k(\epsilon) = \max\{-\frac{1}{2}\log_2\left(4^{-\log N} - 96\log(1 - \epsilon)\right), 2\}$$

which is asymptotically independent of N, according to [38].

To apply this method, first we define $||A||_F = \sqrt{\sum_{i,j} A_{ij}^2}$ and define the new variable k = j + (i-1)N as above. Suppose that the entries $\{A_{ij}\}_{i,j=1}^N$ are positive (we will show how to deal with negative entries subsequently), and there is some positive integrable function $f: [0,1] \longrightarrow (0,1]$ such that: $f(\frac{k}{MN}) = f(\frac{j+(i-1)N}{MN}) = \frac{1}{||A||_F} A_{ji}$, then the method of [38] can be used to prepare the state

$$\sum_{k=1}^{MN} f(\frac{k}{MN}) |k\rangle = \sum_{i,j=1}^{M,N} \frac{1}{||A||_F} A_{ji} |k\rangle = \frac{1}{||A||_F} \sum_{i,j=1}^{N,M} A_{ji} |j\rangle |i\rangle.$$
 (J8)

Again, we recall what we commented earlier, that in reality there can be many possible choice for f. One way to obtain a function f as desired will be discussed in Appendix J3 (see paragraph above Appendix K).

Given the procedure that prepares the state above, then by executing the same procedure as below Eqn. J4, the block-encoding of $\frac{1}{||A||_F^2}A^{\dagger}A$ can be obtained. As the last and optional step, an application of Lemma 6 with the scaling factor $\frac{||A||_F^2}{MN}$ can be used to transform the block-encoded operator

$$\frac{1}{||A||_F^2}A^{\dagger}A \longrightarrow \frac{1}{MN}A^{\dagger}A.$$

Provided that the circuit complexity for preparing $\frac{1}{||A||_F} \sum_{i,j=1}^{N,M} A_{ij} |j\rangle |i\rangle$ is $\mathcal{O}(MN)$, and Lemma 15 uses this state preparation procedure 1 more time, the complexity for obtaining the block-encoding of the operator above is $\mathcal{O}(\log MN)$.

Now we turn our attention to the case where A contains both positive and negative entries. Define $||A^+||_F = \sqrt{\sum_{ij,A_{ij} \geq 0} A_{ij}^+}$ and $|||A^-||_F = \sqrt{\sum_{ij,A_{ij} < 0} A_{ij}^2}$. We consider state:

$$|\phi_{+}\rangle = \frac{1}{||A^{+}||_{F}} \sum_{ij,A_{ij} \geq 0} A_{ij} |j\rangle |i\rangle$$

$$|\phi_{-}\rangle = \frac{1}{||A^{-}||_{F}} \sum_{ij,A_{ij} < 0} A_{ij} |j\rangle |i\rangle$$
(J9)

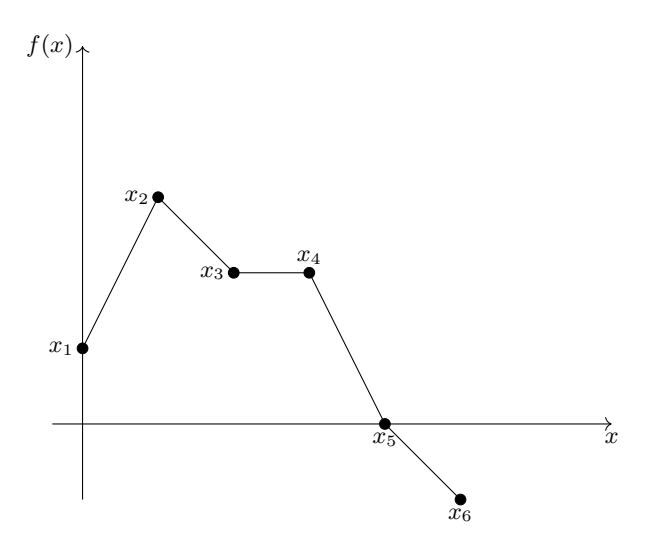


FIG. 2: Simple illustration of the general idea behind our state preparation for $|\Phi\rangle$ indicated at the beginning. We promote x_i to a point on the (x,y) plan with its x coordinate being the index i of x_i , and y being the value x_i . Es each amplitude x_i is randomly chosen from \mathbb{F}_p , it can be seen that $\frac{-p+1}{2} \leq x_i \leq \frac{p-1}{2}$. By connecting these points $\{x_i\}_{i=1}^6$, a piecewise-linear function is formed.

The state $|\phi_{+}\rangle$ has nonnegative entries, so it can be efficiently prepared via the procedure mentioned earlier. Let U_{+} denotes the unitary that prepare this state $|\phi_{+}\rangle$, i.e.,, $U_{+}|0\rangle^{\log MN} = |\phi_{+}\rangle$. Regarding the state $|\phi_{-}\rangle$, we consider the state $-|\phi_{-}\rangle = \frac{1}{||A^{-}||_{F}} \sum_{ij,A_{ij}<0} (-A_{ij})|j\rangle|i\rangle$. Because $A_{ij}<0$, so $-A_{ij}>0$, which is positive. Therefore, the state $-|\phi_{-}\rangle$ can be prepared, with the corresponding preparation unitary U_{-} . Then it can be seen that the first column of U_{+} and U_{-} are $|\phi_{+}\rangle$ and $-|\phi_{-}\rangle$, respectively. Lemma 5 can be used to construct the block-encoding of

$$\frac{||A^+||_F}{||A||_F}U_+ - \frac{||A^-||_F}{||A||_F}U_- \tag{J10}$$

which has the first column to be:

$$\frac{||A^{+}||_{F}}{||A||_{F}}|\phi_{+}\rangle + \frac{||A^{-}||_{F}}{||A||_{F}}|\phi_{-}\rangle = \frac{1}{||A||_{F}} \left(\sum_{ij,A_{ij} \geq 0} A_{ij} |j\rangle |i\rangle + \sum_{ij,A_{ij} < 0} A_{ij} |j\rangle |i\rangle \right). \tag{J11}$$

which is exactly $\frac{1}{||A||_F} \sum_{i,j=1}^{N,M} A_{ij} |j\rangle |i\rangle$. By applying this unitary to $|0\rangle^{\log MN}$, we obtain the desired state. Then we can proceed the same procedure as outlined earlier to obtain the block-encoding of $\frac{1}{MN} A^{\dagger} A$, with the complexity being the same, of order $\mathcal{O}(\log MN)$.

In addition, we remark that in the same work [38], the authors also proposed a variational approach to prepare the desired state. As empirically demonstrated, their variational approach can work well in practice without a lot of training time.

Approach 3 – based on [40]. At the same time, the method in [40] proposes another variational approach to prepare a state of the form $\frac{1}{||x||}\sum_{i=1}^{N}x_i|i\rangle$ where $||x||^2 = \sum_{i=1}^{N}x_i^2$. As analyzed and numerically verified in [40], a parameterized quantum circuit of complexity $\mathcal{O}(l\log N)$ (where $l=\mathcal{O}(1)$) is sufficient to prepare the desired state, even without error tolerance. In addition, the maximum number of ancilla qubits is $\mathcal{O}(1)$. Therefore, a direct application of this state preparation method allows us to prepare the state $\frac{1}{||A||_F}\sum_{i,j=1}^{N,M}A_{ij}|j\rangle|i\rangle$. The procedure for obtaining the block-encoding $\frac{1}{||A||_F^2}A^{\dagger}A$, and then $\frac{1}{MN}A^{\dagger}A$ is straightforward described in the previous paragraph, achieving the same complexity.

2. Application to our case: $A \equiv \partial_r$

Now we return to the context of Lemma 2, where the role of matrix A above is replaced by the boundary operator ∂_r , which has dimension dim $\partial_r = |\mathcal{S}_{r-1}||\mathcal{S}_r|$. By defining an arbitrary (preferably smooth) function that satisfies

$$f(\frac{j+(i-1)N}{|S_{r-1}||S_r|}) = (\partial_r)_{ij} \in \{-1, 0, 1\}$$

, then the method of [39] as well as the procedure outlined above is directly applicable so as to obtain the block-encoding of $\frac{1}{\dim \partial_r} \partial_r^T \partial_r$. This block-encoding procedure has total circuit complexity $\mathcal{O}(\log |S_r||S_{r-1}|)$ and in particular, using $\mathcal{O}(1)$ ancilla qubits only.

On the other hand, instead of using [39], we can use the state preparation method in [38, 59] by defining a positive integrable function that has values

$$f(\frac{j+(i-1)N}{|\mathcal{S}_{r-1}| |\mathcal{S}_r|}) = \frac{1}{||\partial_r||_F} (\partial_r)_{ij} \in \{-\frac{1}{||\partial_r||_F}, 0, \frac{1}{||\partial_r||_F}\}.$$

The circuit complexity of this approach is $\mathcal{O}\left(2^{k(\epsilon)}\right)$ with $k(\epsilon)$ defined earlier, and in addition, this approach does not use any ancilla qubits. Last, the variational approach of [38] or [40] can also be applied, using a quantum circuit of complexity $\mathcal{O}\left(\log|\mathcal{S}_r-1||\mathcal{S}_r|\right)$ and maximally extra $\mathcal{O}(1)$ ancilla qubits.

Thus, overall, we have completed the proof of Lemma 2. In the following, we will proceed to the proof of Lemma 1. In particular, we will show a route to enhance the state preparation methods previously discussed.

3. Proof of Lemma 1 and a followed-up byproduct

Recall that our goal is to construct a unitary that prepares the following state:

$$|\Phi\rangle = \frac{1}{||\mathbf{x}||} \sum_{i=0}^{N-1} x_i |i\rangle \tag{J12}$$

where $||a|| = \sqrt{\sum_{i=0}^{N-1} a_i^2}$ and each a_i is probabilistically drawn from the finite set:

$$\mathbb{F}_p \equiv \left(\frac{-(p-1)}{2}, \dots, -1, 0, 1, \dots \frac{p-1}{2}\right) \tag{J13}$$

with p being a prime number. It is easy to see that once the values of $\{x_i\}$ are provided, this is just the corollary of the state preparation methods discussed earlier. In the following, we discuss two important practical aspects of state preparation methods [39] and [38].

First, as we described earlier, the method of [39] involves ancilla measurement and post-selection. Thus, the overall complexity contains the factor $\mathcal{O}\left(\frac{\sqrt{N}}{||\mathbf{x}||}\right) = \mathcal{O}\left(\sqrt{\frac{N}{||\mathbf{x}||^2}}\right)$, which can be large if $||\mathbf{x}||$ is small. In the next appendix, we will provide a more detailed analysis, showing that the expectation value of $||\mathbf{x}||^2$ is of order $\mathcal{O}(N)$ and thus guaranties the complexity of this step to be $\mathcal{O}(1)$, on average.

Second, to apply the method of [39] and [38], we need a function that, respectively, satisfies $f(\frac{i}{N}) = x_i$ (for [39]) and $f(\frac{x}{N}) = \frac{x_i}{||\mathbf{x}||}$ (for [38]). In practice, we are provided with values of x_i only. The challenge then is: how to effectively choose the function f as desired? Although there can be many choices, and hence, probably many ways to find a good function, we propose the following route. First, we promote the points $\{x_i\}_{i=1}^N$ to the x-y plane, with corresponding coordinates $\{(i,x_i)\}_{i=1}^N$. We then connect these points consecutively from lower indexes to higher ones. The result is a piecewise-linear function, e.g., see Fig 2 for a simple illustration with 6 points. Then we can take advantage of existing results in approximating the piecewise-linear function [41, 42, 44] to obtain the function f as desired. Therefore, we have provided a justification for what we have stated earlier. In the context of **Approach 1** and **Approach 2**, we can applied the route we just described to find the desired f, so as to prepare the state $\sim \sum_{i,j=1}^{N,M} A_{ij} |j\rangle |i\rangle$.

As a final remark, piecewise-linear function is still continuous, and thus the rigorous performance guaranty of [38] still holds. In addition, piecewise-linear function in our case is also piecewise-smooth, so the method [39] can still be applicable. As a byproduct, what we describe above is an effective way to expand the capability of state preparation methods [38] and [39] in practice.

Appendix K: Analysis of the norm ||x||

We begin with the following statement, with its proof provided subsequently:

Lemma 16. Let $\{x_i\}_{i=1}^N$ be i.i.d. entries randomly drawn from $\mathbb{F}_p \equiv \{-\frac{p-1}{2}, -\frac{p-1}{2}+1, ..., -1, 0, 1, \frac{p-1}{2}+1, \frac{p-1}{2}\}$ with probability $\frac{1}{p}$. Define $||\mathbf{x}|| = \sqrt{\sum_{i=1}^{N} x_i^2}$. Then we have

• (Weak version) For some $S \in \mathbb{R}_+$ and $S^2 \geq \frac{N(p^2-1)}{12}$, the probability that $||\mathbf{x}|| \leq S$ is:

$$\Pr(||\boldsymbol{x}|| \le S) \ge 1 - \frac{N\left(\frac{p^4}{180} - \frac{p^2}{36} + \frac{1}{45}\right)^2}{N\left(\frac{p^4}{180} - \frac{p^2}{36} + \frac{1}{45}\right)^2 + (S^2 - \frac{N(p^2 - 1)}{12})^2}$$
(K1)

• (Stronger version) For any $S \in \mathbb{R}_+$:

$$\Pr(||\mathbf{x}|| \le S) \ge \Phi\left(\frac{S^2 - \frac{N(p^2 - 1)}{12}}{\sqrt{N}\left(\frac{p^4}{180} - \frac{p^2}{36} + \frac{1}{45}\right)}\right) - \frac{0.56(p - 1)^6}{2^6\left(\frac{p^4}{180} - \frac{p^2}{36} + \frac{1}{45}\right)^3\sqrt{N}}$$
(K2)

where Φ is the standard normal CDF.

Proof: Our proof makes use of well-known results from probability theory & statistics. We define the following variable:

$$x_i \in \mathbb{F}_p$$
 (K3)

$$Z_i = x_i^2 \tag{K4}$$

$$||\mathbf{x}||^2 = \sum_{i=1}^N Z_i \tag{K5}$$

For convenience, we denote $\mathbb{F}_p \equiv \{-\frac{p-1}{2} + k\}$ for k = 0, 1, ..., p-1. Then it can be seen that:

$$\Pr(x_i = -\frac{p-1}{2} + k) = \frac{1}{p}$$
 (K6)

for any i = 1, 2, ..., N and k = 0, 1, ..., p - 1. We compute the mean and the variance of Z_i as follows:

$$\mathbb{E}(Z_i) = \sum_{k=0}^{p-1} \Pr(\mathbf{x}_i = -\frac{p-1}{2} + \mathbf{k}) \left(-\frac{p-1}{2} + \mathbf{k} \right)^2$$
 (K7)

$$=\sum_{k=0}^{p-1} \frac{1}{p} \left(-\frac{p-1}{2} + k \right)^2 \tag{K8}$$

$$=\frac{p^2 - 1}{12} \tag{K9}$$

$$Var(Z_i) = \sum_{k=0}^{p-1} Pr(x_i = -\frac{p-1}{2} + k) \frac{\left(\left(-\frac{p-1}{2} + k\right)^2 - \mathbb{E}(Z_i)\right)^2}{N-1}$$
(K10)

$$=\frac{p^4}{180} - \frac{p^2}{36} + \frac{1}{45} \tag{K11}$$

With regard to $||\mathbf{x}||^2 = \sum_{i=1}^N Z_i$, we have the following:

$$\mathbb{E}(||\mathbf{x}||^2) = \sum_{i=1}^{N} \mathbb{E}(Z_i)$$
 (K12)

$$= N \frac{p^2 - 1}{12} \tag{K13}$$

$$\operatorname{Var}(||\mathbf{x}||^2) = N \sum_{i=1}^{N} \operatorname{Var}(Z_i)$$
(K14)

$$= N\left(\frac{p^4}{180} - \frac{p^2}{36} + \frac{1}{45}\right) \tag{K15}$$

We also point out that:

$$\Pr(||\mathbf{x}|| \le S) = \Pr(||\mathbf{x}||^2 \le S^2).$$
 (K16)

The weak version of the lemma above is a consequence of the one-sided Chebysev-Cantelli inequality, which states that, for a random variable Y drawn from a probability distribution with mean μ and variance σ , it holds that:

$$\Pr(Y \ge \mu + t) \le \frac{\sigma^2}{\sigma^2 + t^2} \tag{K17}$$

In our case, we need to replace:

$$Y = ||\mathbf{x}||^2 \tag{K18}$$

$$\mu = \mathbb{E}(||\mathbf{x}||^2) = N \frac{p^2 - 1}{12} \tag{K19}$$

$$\sigma^2 = \text{Var}(||\mathbf{x}||^2) = N\left(\frac{p^4}{180} - \frac{p^2}{36} + \frac{1}{45}\right)$$
 (K20)

$$t = S^2 - \mu \tag{K21}$$

Then we have:

$$Pro(||\mathbf{x}||^2 \ge S^2) \le \frac{\sigma^2}{\sigma^2 + (S^2 - \mathbb{E}(||\mathbf{x}||)^2)}$$
(K22)

which implies that:

$$\operatorname{Pro}(||\mathbf{x}||^{2} \leq S^{2}) \geq 1 - \frac{\sigma^{2}}{\sigma^{2} + (S^{2} - \mathbb{E}(||\mathbf{x}||)^{2}}$$
(K23)

$$\geq 1 - \frac{N\left(\frac{p^4}{180} - \frac{p^2}{36} + \frac{1}{45}\right)^2}{N\left(\frac{p^4}{180} - \frac{p^2}{36} + \frac{1}{45}\right)^2 + (S^2 - \frac{N(p^2 - 1)}{12})^2}$$
(K24)

thus completing the proof of the weak version of Lemma 16.

The strong version, on the other hand, is a consequence of the Berry-Esseen-type normal bound. It states that for a random variable Y drawn from a probability distribution with mean μ , variance σ^2 , defining the variable $X = \frac{S^2 - \mu}{\sigma}$, then it holds that:

$$\Pr(Y \le S^2) \ge \Phi(x) - \frac{C\rho}{\sigma^3/N} \tag{K25}$$

where $C \leq 0.56$ is a constant, and $\rho \equiv \mathbb{E}(|Z_i - \mathbb{E}(Z_i)|)^3$. Again, we replace:

$$Y = ||\mathbf{x}||^2 \tag{K26}$$

$$\mu = \mathbb{E}(||\mathbf{x}||^2) = N \frac{p^2 - 1}{12} \tag{K27}$$

$$\sigma^2 = \text{Var}(||\mathbf{x}||^2) = N\left(\frac{p^4}{180} - \frac{p^2}{36} + \frac{1}{45}\right)$$
 (K28)

Now we consider specifically the term $\rho \equiv \mathbb{E}(|Z_i - \mathbb{E}(Z_i)|)^3$, showing that it is upper bounded. We have that:

$$\mathbb{E}(|Z_i - \mathbb{E}(Z_i)|)^3 = \sum_{k=0}^{p-1} \Pr(\mathbf{x}_i = -\frac{p-1}{2} + \mathbf{k}) \left| \left(-\frac{p-1}{2} + \mathbf{k} \right) \right|^2 - \frac{p^2 - 1}{12} \right|^3$$
 (K29)

$$=\sum_{k=0}^{p-1} \frac{1}{p} \left| \left(-\frac{p-1}{2} + k \right) \right|^2 - \frac{p^2 - 1}{12} \right|^3 \tag{K30}$$

We observe that, for all k:

$$\left(-\frac{p-1}{2}+k)\right)^2 - \frac{p^2-1}{12} \le \left(\frac{p-1}{2}\right)^2 \tag{K31}$$

Thus:

$$\sum_{k=0}^{p-1} \frac{1}{p} \left| \left(-\frac{p-1}{2} + k \right) \right|^2 - \frac{p^2 - 1}{12} \right|^3 \le \sum_{k=0}^{p-1} \frac{1}{p} \left(\frac{p-1}{2} \right)^6 \tag{K32}$$

$$\leq \left(\frac{p-1}{2}\right)^6 \tag{K33}$$

So we have:

$$\rho \equiv \mathbb{E}(|Z_i - \mathbb{E}(Z_i)|)^3 \le \left(\frac{p-1}{2}\right)^6 \tag{K34}$$

So from the inequality:

$$\Pr(Y \le S^2) \ge \Phi(x) - \frac{C\rho}{\sigma^3/N} \tag{K35}$$

we can deduce that:

$$\Pr(||\mathbf{x}||^2 \le S^2) \ge \Phi\left(\frac{S^2 - \frac{N(p^2 - 1)}{12}}{\sqrt{N}\left(\frac{p^4}{180} - \frac{p^2}{36} + \frac{1}{45}\right)}\right) - \frac{0.56(p - 1)^6}{2^6\left(\frac{p^4}{180} - \frac{p^2}{36} + \frac{1}{45}\right)^3\sqrt{N}}$$
(K36)

which is inherently equivalent to:

$$\Pr(||\mathbf{x}|| \le S) \ge \Phi\left(\frac{S^2 - \frac{N(p^2 - 1)}{12}}{\sqrt{N}\left(\frac{p^4}{180} - \frac{p^2}{36} + \frac{1}{45}\right)}\right) - \frac{0.56(p - 1)^6}{2^6\left(\frac{p^4}{180} - \frac{p^2}{36} + \frac{1}{45}\right)^3\sqrt{N}}$$
(K37)